



# The NASA AfriSAR campaign: Airborne SAR and lidar measurements of tropical forest structure and biomass in support of current and future space missions

Temilola Fatoyinbo<sup>a,\*</sup>, John Armston<sup>b</sup>, Marc Simard<sup>c</sup>, Sassan Saatchi<sup>c</sup>, Michael Denbina<sup>c</sup>, Marco Lavalley<sup>c</sup>, Michelle Hofton<sup>b</sup>, Hao Tang<sup>b,r</sup>, Suzanne Marselis<sup>b</sup>, Naiara Pinto<sup>c</sup>, Steven Hancock<sup>d</sup>, Brian Hawkins<sup>c</sup>, Laura Duncanson<sup>b</sup>, Bryan Blair<sup>a</sup>, Christy Hansen<sup>a</sup>, Yunling Lou<sup>c</sup>, Ralph Dubayah<sup>b</sup>, Scott Hensley<sup>c</sup>, Carlos Silva<sup>b,e</sup>, John R. Poulsen<sup>f</sup>, Nicolas Labrière<sup>g</sup>, Nicolas Barbier<sup>h</sup>, Kathryn Jeffery<sup>i</sup>, David Kenfack<sup>j</sup>, Memiaghe Herve<sup>k</sup>, Pulchérie Bissiengou<sup>l</sup>, Alfonso Alonso<sup>j</sup>, Ghislain Moussavou<sup>m</sup>, Lee T.J. White<sup>i,n</sup>, Simon Lewis<sup>o,p</sup>, Kathleen Hibbard<sup>q</sup>

<sup>a</sup> NASA Goddard Space Flight Center, Greenbelt, MD, USA

<sup>b</sup> Department of Geographical Sciences, University of Maryland, College Park, USA

<sup>c</sup> Jet Propulsion Laboratory, California Institute of Technology, Pasadena, CA, USA

<sup>d</sup> School of Geosciences, University of Edinburgh, United Kingdom

<sup>e</sup> School of Forest, Fisheries, and Geomatics Sciences (FFGS), University of Florida, Gainesville, FL 32611, United States of America

<sup>f</sup> Nicholas School of the Environment, Duke University, USA

<sup>g</sup> Laboratoire Évolution et Diversité Biologique, UMR 5174 (CNRS/IRD/UPS), France

<sup>h</sup> AMAP, IRD, CNRS, INRA, Univ Montpellier, CIRAD, Montpellier, France

<sup>i</sup> School of Natural Sciences, University of Stirling, FK9 4LA, United Kingdom

<sup>j</sup> Center for Tropical Forest Science—Forest Global Earth Observatory, Smithsonian Tropical Research Institute, Smithsonian Institution, Washington, DC, United States

<sup>k</sup> Institut de Recherche en Ecologie Tropicale (IRET), CENAREST, Libreville, Gabon

<sup>l</sup> Institut de Pharmacopée et de Médecine Traditionnelle (Herbier National du Gabon), CENAREST, Libreville, Gabon

<sup>m</sup> Agence Gabonaise d'Études et d'Observations Spatiales, Libreville, Gabon

<sup>n</sup> Agence Nationale des Parcs Nationaux, Libreville, Gabon

<sup>o</sup> Department of Geography, University College London, London, United Kingdom

<sup>p</sup> School of Geography, University of Leeds, Leeds, United Kingdom

<sup>q</sup> NASA Headquarters, Washington, DC, USA

<sup>r</sup> Department of Geography, National University of Singapore, Singapore

## ARTICLE INFO

Editor: Jing M. Chen

### Keywords:

AfriSAR  
LVIS  
UAVSAR  
GED  
NISAR  
BIOMASS  
Gabon  
Central Africa  
Airborne Campaigns  
Forest Structure  
Lidar  
SAR

## ABSTRACT

In 2015 and 2016, the AfriSAR campaign was carried out as a collaborative effort among international space and National Park agencies (ESA, NASA, ONERA, DLR, ANPN and AGEOS) in support of the upcoming ESA BIOMASS, NASA-ISRO Synthetic Aperture Radar (NISAR) and NASA Global Ecosystem Dynamics Initiative (GED) missions. The NASA contribution to the campaign was conducted in 2016 with the NASA LVIS (Land Vegetation and Ice Sensor) Lidar, the NASA L-band UAVSAR (Uninhabited Aerial Vehicle Synthetic Aperture Radar). A central motivation for the AfriSAR deployment was the common AGBD estimation requirement for the three future spaceborne missions, the lack of sufficient airborne and ground calibration data covering the full range of ABGD in tropical forest systems, and the intercomparison and fusion of the technologies.

During the campaign, over 7000 km<sup>2</sup> of waveform Lidar data from LVIS and 30,000 km<sup>2</sup> of UAVSAR data were collected over 10 key sites and transects. In addition, field measurements of forest structure and biomass were collected in sixteen 1-hectare sized plots. The campaign produced gridded Lidar canopy structure products, gridded aboveground biomass and associated uncertainties, Lidar based vegetation canopy cover profile products, Polarimetric Interferometric SAR and Tomographic SAR products and field measurements. Our results

\* Corresponding author at: 8800 Greenbelt Drive, Greenbelt, MD 20771, USA.

E-mail address: [lola.fatoyinbo@nasa.gov](mailto:lola.fatoyinbo@nasa.gov) (T. Fatoyinbo).

<https://doi.org/10.1016/j.rse.2021.112533>

Received 18 June 2020; Received in revised form 19 May 2021; Accepted 22 May 2021

Available online 7 July 2021

0034-4257/Published by Elsevier Inc. This is an open access article under the CC BY license (<http://creativecommons.org/licenses/by/4.0/>).

showcase the types of data products and scientific results expected from the spaceborne Lidar and SAR missions; we also expect that the AfriSAR campaign data will facilitate further analysis and use of waveform lidar and multiple baseline polarimetric SAR datasets for carbon cycle, biodiversity, water resources and more applications by the greater scientific community.

## 1. Introduction: the need for multi-sensor forest structure datasets

Following the urgent need for improved mapping of vegetation structure (Le Toan et al., 2011) to better quantify global carbon stocks and fluxes from land use change (Houghton, 2005) and impacts on ecosystem services and forest resources (Bustamante et al., 2016), NASA and ESA have developed three spaceborne missions – NASA Global Ecosystems Dynamics Investigation (GEDI, Dubayah et al., 2020), NASA-ISRO Synthetic Aperture Radar Mission (NISAR, Rosen et al., 2016) and ESA BIOMASS (Quegan et al., 2019) - to be launched between 2018 and 2022. By virtue of the different sensitivities to forest structure combined with overlapping coverage at different geographic and time scales, NISAR, GEDI and BIOMASS are slated for new remote sensing analysis and scientific discovery that were not possible to date or with each mission alone. In particular, the fusion of data from these three missions, which will be freely and publicly available, will provide scientific opportunities to further our understanding of ecosystem processes from the scale of anthropogenic disturbance to the global scale. An overview of the main expected mission parameters is shown in Table 1.

GEDI is a geodetic laser altimeter and waveform lidar instrument built and operated by NASA and University of Maryland. The GEDI mission launched on December 5th, 2018 and deployed on the International Space Station (ISS), with the aim of measuring forest structure and biomass within the ISS coverage window of  $\pm 51.6$  degrees latitude (Dubayah et al., 2020; Duncanson et al., 2020). The GEDI mission provides canopy height and Aboveground Biomass Density (AGBD) samples within 25 m footprints and a wall-to-wall gridded data products at 1 km resolution. The GEDI mission's strengths lie in the penetration capability of GEDI's near infrared lasers (1064 nm wavelength) and the near-continuous recording of the returned signal, providing the most accurate vertical samples of canopy structure from space. The spatial distribution of GEDI footprints is dense in tropical biomes (8 tracks separated by  $\sim 600$ -m across track with footprints spaced  $\sim 60$ -m along track) but no observations will be generated at high-latitudes ( $>51.5$  degrees) due to the ISS orbit.

The NASA-ISRO Synthetic Aperture Radar Mission (NISAR) is a three-year joint US-India L- and S-band SAR mission to be launched in 2023 with scientific applications in the solid earth, cryosphere, hydrosphere and ecosystem sciences (Rosen et al., 2017). NISAR will provide global, cloud-free, wall-to-wall L-band SAR observations with two polarizations (HH and HV) at 12.5 m resolution, with a 12 day repeat and approximately 30 observations per year (NISAR, 2018). One of the mission objectives is to map woody vegetation disturbance, recovery

and AGBD up to  $100 \text{ Mg ha}^{-1}$  at the 1 ha scale. NISAR's primary limitation for mapping of forest structure lies in the reduced sensitivity of L-band backscatter to AGBD above approximately  $100 \text{ Mg/ha}$  (Yu and Saatchi, 2016). This limits accurate AGBD mapping in most dense tropical, subtropical and temperate forests if backscatter alone is used.

The European Space Agency's BIOMASS Mission is a 5-year P-band SAR mission (435 Mz) to be launched in October 2022 with the primary objectives of mapping forest AGBD and height at 200 m spatial resolution and disturbance at 50 m spatial resolution (Carreiras et al., 2017; Le Toan et al., 2011). The ESA BIOMASS mission will collect data in fully polarimetric, repeat-pass interferometric and tomographic modes to produce repeated measurements of forest height as well as AGBD during its 5-year mission life (Quegan et al., 2019). These maps are expected to be more accurate in higher AGBD ecosystems than those produced by other SAR missions, due to higher P-band penetration into the canopy compared to shorter wavelengths such as L, C, X or S-band and, more importantly, due to the missions' capability to support Polarimetric InSAR and Tomographic SAR. However, the BIOMASS mission will only acquire data over tropical and subtropical regions worldwide due to the International Telecommunication Union–Radiocommunications restrictions over North America and Europe (Carreiras et al., 2017).

In anticipation of the three missions, there was a need for field and airborne measurements of forest structure and condition, as well as new forest structure retrieval algorithms across a wide range of tropical forest conditions. As a result the European Space Agency (ESA), United States National Aeronautics and Space Agency (NASA), French Aerospace Lab (Office National d'Etudes et de Recherches Aéronautiques; ONERA), German Space Agency (Deutsches Zentrum für Luft-und Raumfahrt; DLR), Gabonese National Park Agency (Agence Nationale des Parcs Nationaux; ANPN), the Gabonese Earth Observation Agency (Agence Gabonaise de l'Etude et Observation Spatiale; AGEOS) and multiple international University partners collaborated on the AfriSAR campaign, to acquire coincident calibration and validation datasets that would facilitate comparison between the airborne, field and spaceborne data. It follows NASA's previous regional field campaigns, such as 1994 and 1996 Boreal Ecosystem-Atmosphere Study (BOREAS), the 2001 Large Scale Biosphere-Atmosphere Experiment in Amazonia (LBA-ECO) and the 2015 Arctic-Boreal Vulnerability Experiment (ABOVE), and ESA's TropiSAR in combining remote-sensing techniques and ground-based experiments to assess ecosystem structure and change in responses to anthropogenic and environmental drivers.

The primary aim of the AfriSAR campaign was to collect ground, airborne SAR and airborne Lidar data for the development and evaluation of forest structure and AGBD retrieval algorithms and GEDI, NISAR and BIOMASS sensor calibration and validation. The campaign consisted

**Table 1**  
Overview of the GEDI, NISAR and BIOMASS expected mission parameters.

	GEDI	NISAR	BIOMASS
Type	Waveform Lidar	L-band SAR	P-band SAR
Coverage	$\sim \pm 51.6$ degrees	Global	South America, Africa, Asia, Australia
Launch date	Dec 5, 2018	2022	2022
Min. Mission length	2 years	3 years	5 years
Repeat coverage	None	Every 12 days	Every 3 days
Resolution	25 m footprint 1 km gridded data	12.5 m SLC 12.5 $\times$ 12.5 GRD	30 m SLC 50 m gridded Disturbance 200 m gridded Height and AGBD product
AGB range	all	$<100 \text{ Mg ha}^{-1}$	all
AGBD Uncertainty	$<20 \text{ Mg ha}^{-1}$ or 20% standard error, whichever is greater, for 80% of 1 km cells	20% up to $100 \text{ Mg ha}^{-1}$	20% for AGBD $>50 \text{ Mg ha}^{-1}$ 10 $\text{Mg ha}^{-1}$ for AGBD $<50 \text{ Mg ha}^{-1}$

of two deployments, the first deployment in 2015 focused only on ESA BIOMASS calibration with the ONERA SETHI P- and L- band SAR system; the second in 2016 included the NASA deployment, with the NASA LVIS (Land Vegetation and Ice Sensor) Lidar, the NASA L-band UAVSAR and the DLR L- and P-band F-SAR system; during both deployments AGEOS and ANPN collaborated on site selection, coordination and field measurements. The objectives of the AfriSAR deployments were to:

- 1) Measure forest canopy height, canopy profiles and AGBD under a variety of forest conditions, such as primary and degraded forest, and a variety of forest types, including tropical rainforest, mangroves, forested freshwater wetlands and savannas.
- 2) Acquire detailed measurements of airborne SAR data and Lidar data for validation and cross calibration of NASA and ONERA/DLR instruments and for calibration and validation support of the BIOMASS, NISAR, and GEDI missions.
- 3) Conduct technology demonstrations of joint SAR and Lidar applications for improved measurement of canopy structure and AGBD.

The AfriSAR campaign encompassed both field and airborne missions to study forest structure and AGBD of tropical forests. The ESA and DLR acquisition and analysis have been described in detail in Hajnsek et al. (2016), Wasik et al. (2018) as well as Labrière et al. (2018). In this paper, we focus on the NASA contribution to the AfriSAR campaign and describe the objectives, field measurements and study sites covered. We also provide an overview and analysis of the higher-level NASA AfriSAR data products and in anticipation of similar data products that will result from NISAR and GEDI. In section 2 we describe the targeted field sites and study area. Section 3 provides a detailed overview of the field and airborne data analysis while section 4 describes the methods used to acquire field and airborne canopy structure and AGBD estimates from different sensors and processing techniques, such as PolInSAR, Lidar and Tomographic SAR. In section 5, we present an analysis and comparison of the different data produced by the campaign. Section 6 discusses the broader implications of the airborne campaign for mission algorithm development and existing applications of the data. Finally, in section 7, we discuss the implications of the campaign and present our general conclusions.

## 2. Study area

Gabon was selected as the study area for AfriSAR due to ecological and logistical considerations, as it is a densely forested country with rich structural and functional biodiversity. By area, Gabon is the second most forested tropical country in the world with 88.5% forest cover and 23.5 M ha of forest (Sannier et al., 2014). Its composition roughly follows the precipitation gradient, with mesic equatorial coastal forests in the west and drier Guinean–Congolian lowland forests in the east (Poulsen et al., 2017). Forests are estimated to have the second highest carbon density after Malaysia, with a mean total (above and belowground) carbon density of 164 Mg C ha<sup>-1</sup> (Saatchi et al., 2011). Almost three-quarters (67%) of Gabon's forest is in logging concessions while 30,000 km<sup>2</sup> or 11% of the land areas are protected in 13 national parks that encompass most of the important terrestrial, coastal, and marine ecosystems in the country (Forêt Ressources Management, 2018). Across the country, 31% of the forested areas have been selectively logged, with harvest intensities ranging from 0.4–0.8 trees ha<sup>-1</sup> (Medjibe et al., 2013). Gabon has among the richest wildlife and plant communities in Africa, and up to 20% of its species are endemic to the country. For example, roughly 40% of the world's western lowland gorillas are thought to live in Gabon (Laurance et al., 2006).

The sites imaged as part of the NASA AfriSAR campaign were selected based on preceding ESA acquisitions, the availability of field measurements of forest structure, accessibility and recommendations by experts, most notably the Gabonese National Park Service - Agence Nationale des Parcs Nationaux (ANPN). The four joint ESA/NASA

AfriSAR Sites were Mondah forest, Lopé National Park, Mabounié and Rabi (Fig. 1). The additional NASA AfriSAR sites were Pongara National Park, Akanda National Park, the Gamba Complex and Mouila, as well as two transects flown to capture geographic and climatic variability. See the Supplemental material for a detailed description of the sites.

## 3. Airborne and field data acquisition

LVIS is a medium-altitude imaging laser altimeter designed and developed at the NASA Goddard Space Flight Center to measure vegetation structure, sub canopy ground elevation, and topography of ice sheets and glaciers (Blair et al., 1999). It is also the airborne prototype of the GEDI mission with similar instrument and data specifications. LVIS was flown in Gabon from February 20th to March 8th 2016 on the NASA Langley King Air B-200 at an altitude of 7.3 km (Table 2). The nominal footprint diameter was 22 m with 9 m separation, providing overlapping along track footprints. Both the transmitted and return signals are digitized to provides a true 3D vertical record of intercepted surfaces including the canopy surfaces and underlying ground. From each waveform, canopy height, canopy vertical metrics, and subcanopy topography were derived, relative to the WGS-84 ellipsoid (Blair et al., 1999; Blair and Hofton, 2018). We compared LVIS crossover footprints (areas where two footprints from different acquisitions overlap) to compute horizontal and vertical accuracy of the measurements.

LVIS standard data products include Level 1B and 2B. The Level 1B product contains the geolocated laser return waveforms in HDF5 format. The Level 2 product contains elevation (ground and canopy top) and Relative Height (RH) products derived from the Level 1B file in ASCII text (.TXT) format. LVIS Crossover comparisons showed that the LVIS Level 1B product has an expected horizontal geolocation of 1 m or less (Lope 0.41 m, Mabounié 0.57 m, Mondah 0.99 m, and Rabi 0.5 m) and vertical accuracy of 5 to 10 cm (Blair and Hofton, 2018). More acquisition details and original L1 & L2 data products are available through the National Snow and Ice Data Center DAAC and LVIS website.

UAVSAR is an airborne fully polarimetric L-band (1.26 GHz, 80 MHz bandwidth) Synthetic Aperture Radar (SAR) system designed, built and operated out of the NASA Jet Propulsion Laboratory. The instrument was developed for repeat pass interferometry (InSAR) in support of crustal deformation, polarimetric Interferometric SAR (PolInSAR) and Polarimetric tomography (TomoSAR) to measure forest structure and sub canopy topography (Hensley et al., 2008). It was deployed in Gabon from February 23 through March 8, 2016 on the NASA Gulfstream III aircraft, flying at 12.5 km altitude and equipped with a Precision Autopilot system allowing for flight repeat track acquisition within 5 m of the original flight line. UAVSAR multi-looked complex data resolution is 0.00005556 degrees, or 6.14 m at the equator. The aim of collecting UAVSAR in Gabon was to acquire multiple repeat-pass InSAR acquisitions with varying interferometric baselines and time spans, including mimicking NISAR temporal baselines (Denbina et al., 2018a). The different interferometric baselines are obtained by acquiring repeat flight lines parallel to the first line but displaced vertically (i.e. changing flight altitude) by multiples of 15 m or 20 m (Table 2). This flight configuration was designed to resolve a wide range of forest canopy heights, and flight were nudged vertically by 15 m or 20 m to minimize the variation of the interferometric wavenumber within UAVSAR's imaging swath (i.e. the wavenumber varies more rapidly across the range perpendicular to flight with horizontal baselines).

The vertical baselines collected by UAVSAR were planned considering different objectives for the study areas. For example, the Akanda site was flown repeatedly using the same baseline lengths, in order to provide the data for an in-depth study of temporal decorrelation. The Pongara study area was limited to fewer flight lines due to scheduling. The Lope study area had baselines designed for TomoSAR, with consistent spacing between baselines and a large maximum baseline length. The appropriate baseline lengths were also planned using limited pre-existing knowledge (from lidar and field surveys) of the expected



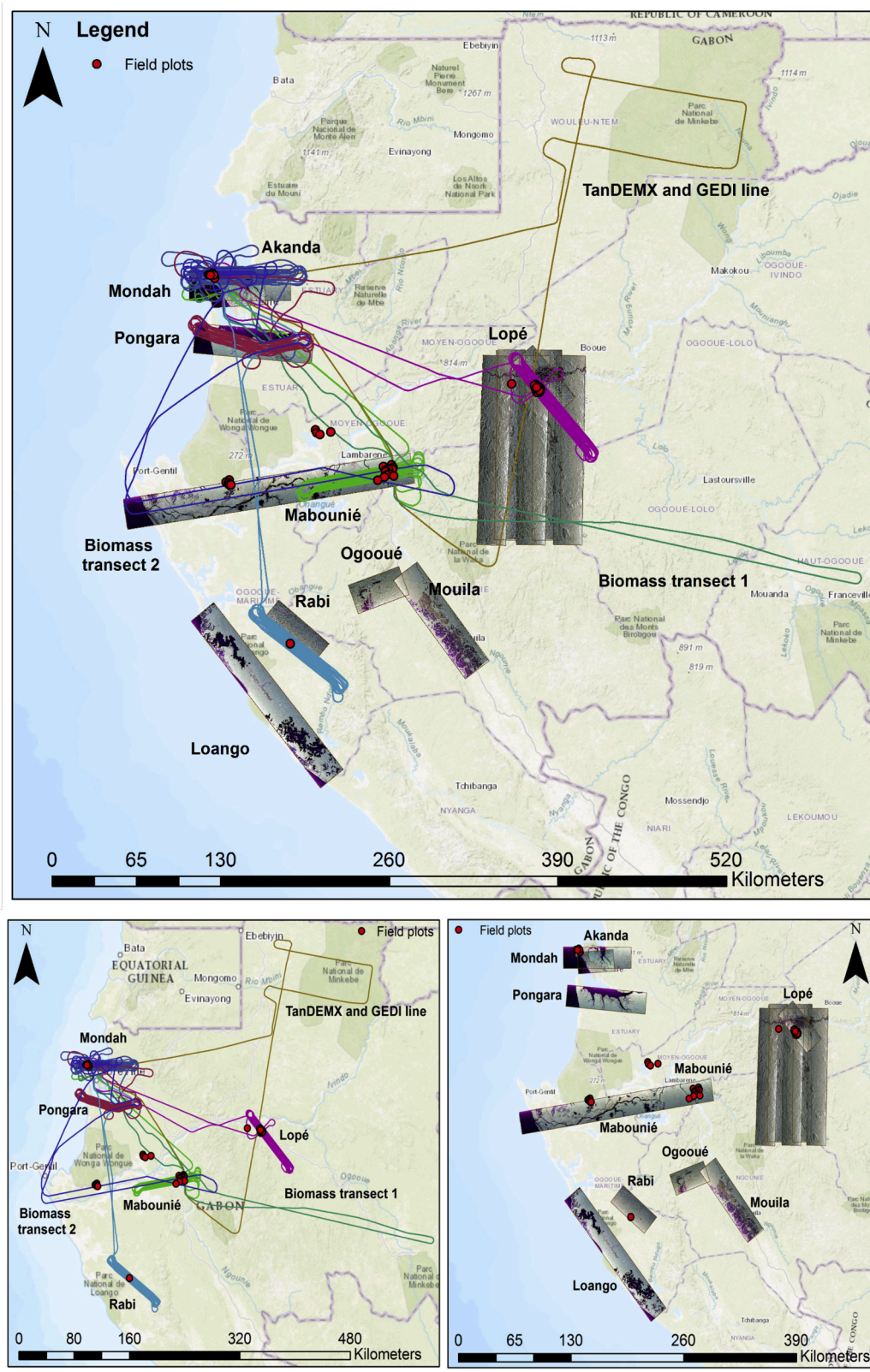


**Fig. 1.** NASA AfriSAR Airborne Acquisitions. A) All LVIS and UAVSAR acquisitions. B and C show LVIS and UAVSAR acquisitions and field data sites separately.

forest heights in each study area. However, some study areas had maximum canopy heights greater than expected, such that the minimum baseline length collected by UAVSAR was insufficient to retrieve the heights of some of the tallest trees (Denbina et al., 2018a).

UAVSAR acquired data in several modes including PolSAR,

Interferometric SAR (InSAR), PolInSAR, Tomographic SAR (TomoSAR), zero-baseline (i.e. exact repeated flight line). The Lopé site was the most extensively covered with up to 9 baselines on two separate dates (Feb 25 and March 8). The two flights were acquired 12 days apart in order to simulate the temporal difference between two NISAR acquisitions.



**Table 2**

LVIS and UAVSAR airborne acquisitions, site names and dates\*

LVIS Acquisitions		
Site Name		Date in 2016
Mabounié		February 20
TanDEM-X transect		February 22
GEDI crossover transect		February 22
Biomass-1 transect		February 23
Lopé		March 2
Pongara		March 4
Rabi		March 7
Mondah and Akanda		March 4
Mondah and Akanda		March 8
Biomass-2 Transect		March 8
UAVSAR acquisitions		
	Vertical Baseline configuration [m]	
Mondah and Akanda	0, 0, 0, 45, 45, 45, 60, 60, 60	March 6
Pongara	0, 20, 45, 105	February 27
Pongara	–	March 6
Lope (North)	0, 20, 40, 60, 80, 100, 120, 0	February 25
Lope (North)	0, 20, 40, 60, 80, 100, 120, 160, 180, 0	March 8
Lope mosaic (entire park)	–	March 1
Rabi	0, 20, 40, 60, 80, 100, 120, 160, 180, 200	February 28
Mouila, Mabounié and Ogooué	0	March 1
Gamba Complex	0	March 6

\* LVIS acquired data on multiple days and flights over several sites. The dates shown here represent primary date at which most of the data over specific sites was collected.

UAVSAR Standard products include full polarimetric (HH-HV-VV-VH) multilook complex (.mlc) gridded geocoded (.grd) data. Additionally, a SLC dataset was produced that includes all of the acquisitions with varying baselines, plus the vertical wavenumber and effective baseline data. The number of repeat passes and baselines are shown in Table 2.

**In Situ:** We established and surveyed field plots in the forested areas in and surrounding the Mondah Forest in collaboration with ANPN. The Mondah plots were spatially distributed in low density forest based on previously developed biomass estimates (Saatchi et al., 2011) and previously flown discrete return Lidar data (Silva et al., 2018) to focus on lower AGBD (<200 Mg AGBD ha<sup>-1</sup>) forests. Sampling was conducted in March 2016 using a modified methodology of the Gabon National Resource Inventory (Poulsen et al., 2017).

The field team established 15 1-ha plots (100 m × 100 m) divided into sixteen 25 × 25 m subplots and recorded the GPS coordinates of all plot and subplot corners. Technicians measured the diameter at breast height (1.3 m) of every tree ≥5 cm and counted the number of trees <5 cm diameter. A botanist identified trees to species or genus. In addition, field teams measured tree heights with a laser hypsometer (TruPulse 200 Hypsometer, Laser Technology, Inc., Centennial, CO, USA), taking three measurements of 55 randomly selected trees per site with 10 trees from each of 5 DBH subclasses (10–20 cm, 21–30 cm, 31–40 cm, 41–50 cm, >50 cm) and the five largest trees. Shrub height was measured at each subplot corner and shrub cover for each quadrant was recorded. Within each subplot, field teams took hemispherical photos at 0.5 m height from the forest floor. For woody vegetation shorter than breast height, a 1 × 1 m mini-plot was randomly set up in each subplot to measure percent ground cover. In addition to these measurements, field teams recorded the following: altitude and orientation of each plot, forest type (primary, secondary or logged), inundation type (never, seasonally or permanently), and presence of disturbances, such as downed trees, fires, elephant or other large animal damage. The field team also noted whether there was evidence of hunting, forest product harvesting, and human trails and stumps.

## 4. NASA AfriSAR Data Products and Algorithms

### 4.1. Data products

Following the release of the standard LVIS and UAVSAR data products, the AfriSAR science team has produced additional Level 3 and 4 data products in line with GEDI and NISAR data products. The aim of producing these products is to promote scientific analyses of the AfriSAR data and advance the calibration and validation between sensors and missions (Table 3). AfriSAR products are versioned and may be improved in the future.

### 4.2. Plot level aboveground biomass density

We estimated AGBD for the Mondah plots using a pantropical allometric model including parameters for tree diameter, height and wood specific density as developed by Chave et al. (2014). We used the R package, BIOMASS, to analyze the plot data (Réjou-Méchain et al., 2017). BIOMASS assigns wood density values to trees, builds a model to predict tree height from DBH using one of five potential functional forms, and propagates errors associated with diameter and wood density measurements, tree height predictions, and the allometric model.

### 4.3. Height and topography products

**LVIS gridded height models and bare earth DEM** were produced for the Lopé, Mondah/Akanda, Pongara, Rabi and Mabounié flightlines from the standard LVIS Level 2 topography and relative height data products distributed for each laser footprint (Blair and Hofton, 2018). The canopy height was determined by the geolocation of the precise timing points along the received waveform. These timing points include the received waveform signal start, end and distinct modes representing reflecting surfaces within each laser footprint. An array of energy percentiles between the signal end (0%) and start (100%) ranging points were then computed, with the relative height (RH) of each percentile bin defined as its elevation minus the elevation of the lowest detected mode (ie the ground) for more detail, see Blair et al. (1999).

The relative height metrics RH25, RH50, RH75, RH90, RH95, RH98, RH99 and RH100 were computed from the lidar waveform. The percentile indicates the relative amount of energy above from the ground. For example, RH50 represents the height below which there is 50% of the lidar return energy. RH98, RH99 and RH100 can be used to represent the top canopy height. The LVIS 25 × 25 m (0.0625 ha) spatial resolution relative height metrics (RH25, RH50, RH75, RH90, RH95, RH98, RH99 and RH100) and bare earth elevation grids were generated from the footprint elevation and height metrics. All shots falling within individual cells according to their ground location were aggregated and statistical moments calculated (mean and standard deviation of values). An ancillary data product describing the number of shots and flightlines used for each grid cell was also generated. The bare earth elevation or Digital Elevation Model (DEM) interpolation approach used the natural neighbor algorithm (Sibson, 1981), which is an efficient interpolation algorithm that requires no local tuning of parameters and has been previously applied to the generation of lidar DEM's over large areas (Fisher et al., 2020). The gridded products cover a smaller spatial extent than the footprint products, since the former include transects and transit flightpaths. All LVIS gridded products use the GeoTIFF format.

**UAVSAR canopy height products** and associated uncertainty maps from multi-baseline Polarimetric Interferometric Synthetic Aperture Radar (PolInSAR) were generated for all sites where multiple interferometric baselines were collected, namely Lopé, Rabi, Pongara and Mondah. The co-registered stacks of UAVSAR SLC images are also distributed as a level 2 product and form basis input layers to derive the PolInSAR height products. Three product variants of the UAVSAR-derived Canopy Height Models (CHM) were generated using different algorithms and implemented using 2 different softwares with potentially

**Table 3**  
AfriSAR data product list.

AfriSAR Data Product Name	Description	Reference
Mondah Forest Tree Species, Biophysical, and Biomass Data, Gabon, 2016	Individual tree, Plot (1 ha) and subplot (0.0625–0.25 ha) AGBD and structure metrics including uncertainty	Fatoyinbo et al., 2018
L1B Geolocated Waveforms	<b>LVIS-based products</b> Geolocated laser return waveforms for each laser footprint	Blair and Hofton, 2018
L2 Elevation and Height Products	Ground and canopy top elevations and relative height metrics describing the vertical distribution of Lidar return energy from the ground.	Blair and Hofton et al., 2018b
Footprint-Level Canopy Cover and Vertical Profile Metrics	Footprint-level products of vertical profiles of canopy cover fraction in 1-m bins, vertical profiles of plant area index (PAI) in 1-m bins, footprint summary data of total recorded energy, leaf area index, canopy cover fraction, and vertical foliage profiles in 10-m bins in Lopé, Mondah/Akanda, Pongara, Rabi and Mabounié.	Tang et al., 2018
Gridded Forest Biomass and Canopy Metrics Derived from LVIS, Gabon, 2016	Gridded version of Canopy cover, canopy heights, bare ground elevation, plant area index (PAI), foliage height diversity (FHD) and respective uncertainties at 25 m resolution in Lopé, Mondah/Akanda and Mabounié.	Armstrong et al., 2020
	Gridded Estimates of aboveground biomass (AGB) and respective uncertainties for four sites in Gabon at 0.25 ha (50 m) resolution derived with field measurements and airborne LiDAR data collected from 2010 to 2016.	Armstrong et al., 2020
Polarimetric SAR Stack	<b>UAVSAR based products</b> Calibrated, co-registered single look complex (SLC) time series data in slant range	Alaska Satellite Facility DAAC
Canopy Height Derived from PolInSAR and Lidar Data	Canopy height and intermediate parameters of the PolInSAR data (including radar backscatter, coherence, and viewing and terrain geometry) from multi-baseline PolInSAR data using the Kapok open-source Python library over Lopé, Pongara, Mondah/Akanda.	Denbina et al., 2018a
	Canopy height derived from a fusion of PolInSAR and LVIS Lidar data over Lopé, Pongara, Mondah/Akanda.	Denbina et al., 2018a
Canopy Structure Derived from PolInSAR and Coherence TomoSAR NISAR tools	Canopy Height, associated uncertainty and intermediate products derived by applying multi-baseline PolInSAR using the PLANT software and Polarimetric Coherence Tomographic SAR (PCT) techniques over Lopé, Mondah and Rabi	Lavalle et al., 2018
Polarimetric Height Profiles by TomoSAR, Lope and Rabi Forests, Gabon, 2016	Canopy height profiles produced using synthetic aperture radar tomography (TomoSAR) over Lopé and Rabi	Hawkins et al., 2018

different interpretations of forest structure and height (e.g. sensitivity to tree density or woody biomass). These three products were produced using:

- 1) the prototype NISAR interferometric processor ISCE (Interferometric Software Computing Environment) and the PLANT toolbox (Polarimetric-Interferometric Lab and Analysis Tool) (Lavalle et al., 2018), called CHM<sub>PLANT</sub> from hereon,
- 2) an inversion of the random volume over ground (RVoG) model implemented in Kapok: an open source Python library (Denbina et al., 2018a). This canopy height inversion is called CHM<sub>Kapok</sub> from hereon,
- 3) a fusion approach that inverts the RVoG model using a Support Vector Machine (SVM) machine learning algorithm to estimate the best interferometric baseline for each pixel. The SVM is trained using lidar canopy height data, and attempts to select the interferometric baseline with highest accuracy given the observed PolInSAR coherence characteristics (Denbina et al., 2018a, 2018b), called CHM<sub>fusion</sub> from hereon.

The standard approach used in all three products for estimating canopy heights from multiple baselines starts by calibrating and co-registering the set of available Single Look Complex (SLC) along with generating maps vertical wavenumber ( $k_z$ ), look vector, and latitude and longitude referenced to the WGS84 ellipsoid. The vertical wavenumber represents the sensitivity of the interferometric phase to vertical canopy height, and is dependent on the spatial baseline between the repeat acquisitions as well as the viewing and target geometry (Kugler et al., 2015). The vertical wavenumber determines the suitability of a given baseline to accurately estimate canopy height for a particular true forest height. Different baselines with different vertical wavenumbers can be utilized to produce consistent canopy height inversion accuracy across a wide range of forest heights (Kugler et al., 2015).

The vertical wavenumber maps were computed using the calculated look vector for each pixel, and considering the distortion effects caused by the underlying ground topography, based on the 30 m SRTM DEM. While higher resolution DEMs were available in some areas, none covered the full extents of the UAVSAR acquisitions. The full look vector was used, rather than just the look angle, in order to account for the effect of aircraft attitude including non-zero squint angle.

**UAVSAR CHM<sub>PLANT</sub>** data were produced for Mondah, Rabi and Lopé National Park sites. These were generated with the prototype NISAR interferometric processor ISCE and the PLANT toolbox starting from polarimetric SAR (PolSAR) SLC stacks (Lavalle et al., 2018). This product also includes various intermediate PolInSAR products including canopy and ground coherence maps, mask coherence separation, mask coherence error and location, and merged vertical wavenumber maps. To generate the CHM<sub>PLANT</sub> product, PolInSAR canopy height and uncertainty products were derived using an algorithm based on the random-volume-over-ground (RVoG) (Cloude and Papathanassiou, 2003; Papathanassiou and Cloude, 2004) and its extension, named random-motion-over-ground (RMOG), to include temporal decorrelation (Lavalle and Hensley, 2015), as well as the structured-volume-over-ground (SVoG) models (Cloude et al., 2006). For CHM<sub>PLANT</sub>, a cost function based on the product between mean PolInSAR coherence and RVoG/RMOG-model visible line length (the distance between optimized PolInSAR coherences) was adopted. The merging of interferometric observations from the multiple baselines ensures a good balance between random phase noise, which increases with baseline length due to increased volume decorrelation and lower interferometric coherence, and interferometric sensitivity to structure. It also provides an effective way to partially compensate for temporal decorrelation effects that result from acquiring images of an interferometric pair in repeat-pass modes (i.e. at different time). Masking of very low coherence samples and very small baselines was applied during the multi-baseline merging process depending on the multi-baseline flight configuration and

characteristics of the imaged forests. The associated canopy height uncertainty product represents the standard deviation in meters of  $CHM_{PLANET}$ . More details about the generation of the  $CHM_{PLANET}$  products and the canopy height uncertainty product can be found in Riel et al., 2018.

**The UAVSAR  $CHM_{Kapok}$**  product provides estimates of forest canopy height and uncertainty for study areas in Pongara and Lopé derived with the Kapok software (Denbina et al., 2018a; Denbina et al., 2018b). This dataset also includes various intermediate PolInSAR products including radar backscatter, coherence, and viewing and terrain geometry. Canopy height was derived from the multi-baseline UAVSAR data by inverting the RVoG model. Kapok uses the SLC stack to calculate a multi-look PolInSAR covariance matrix for each pixel in the imagery. Kapok also resamples the available vertical wavenumber, look vector, and geolocation information to have the same dimensions as the multi-looked UAVSAR image stack.

After calculating the multi-look covariance matrix, a coherence optimization procedure was performed to find the PolInSAR coherences with the largest separation in the complex plane, followed by an estimation of the interferometric phase of the ground surface beneath the forest canopy, as in the standard three-stage RVoG model inversion procedure (Cloude and Papathanassiou, 2003). For each pixel, a single interferometric baseline was used for the height inversion, based on the characteristics of the observed coherence region, as described in (Denbina et al., 2018b).  $CHM_{Kapok}$  products were created by solving for the forest canopy height and extinction parameters of the model, ignoring the effects of temporal decorrelation. Pixels with low HV backscatter were masked out to avoid estimating forest heights over water areas and had their canopy height set to zero (i.e., non-forest).  $CHM_{Kapok}$  uncertainty is the standard deviation in meters of the canopy height product  $h_v$ , derived using the same approach as described in Riel et al. (2018).

**UAVSAR  $CHM_{fusion}$** : In addition to the standard PolInSAR canopy height products derived above, experimental UAVSAR and LVIS fusion canopy height products were also generated for the Pongara and Lopé sites as described in Denbina et al., 2018b. For each pixel, the algorithm uses machine learning to choose the interferometric baseline expected to provide the best canopy height estimate. This selection is primarily based on the characteristics of the observed PolInSAR coherence region, in addition to other parameters such as  $k_z$  and radar backscatter. A sparse subset of coincident LVIS RH100 data, similar to the point density expected from the GEDI mission, was used to train the classifier at approximately 250-m spacing in both azimuth and range directions (Denbina et al., 2018b). After training, for each pixel the baseline selected by the classifier was used to invert forest height from the RVoG model, as described in the previous paragraph. This product helps demonstrate the potential of fusing multi-baseline PolInSAR with data from GEDI or other future spaceborne lidar missions.

#### 4.4. Vertical profile products

The AfriSAR vertical canopy structure products were generated using established algorithms on the LVIS data, and more experimental techniques with UAVSAR data.

**LVIS footprint canopy cover metrics and profiles:** Footprint-level canopy structure products were generated for the Lopé, Mondah/Akanda, Pongara, Rabi and Mabounié flight lines using established techniques (Tang et al., 2018). Products generated are:

1) Vertical profiles of canopy cover fraction (CCF) in 1 m vertical bins. Canopy cover fraction is defined as  $1 - P_{gap}(z, \theta)$ , where  $z$  and  $\theta$  are zero and  $P_{gap}$  is the directional gap probability (Tang and Armston, 2019). This is equivalent to the probability that the ground surface is directly visible at the nadir view of LVIS.

2) Vertical profiles of plant area index  $PAI(z)$  between the top of canopy ( $z = H_{max}$ ) and the ground ( $z = 0$ ), with a vertical bin size of 1 m.  $PAI$  is defined as one half of the total plant element area per unit ground surface ( $m^2 m^{-2}$ ; (Gower and Norman, 1991).

3) Footprint summary data of total recorded energy, PAI, CCF, and vertical plant area volume density (PAVD,  $m^2 m^{-3}$ ) profiles in 10 m vertical bins (i.e. 0–10, 10–20, 20–30 and above), and foliage height diversity (FHD) - a canopy structural index that describes the vertical heterogeneity of the PAVD profile (MacArthur and Horn, 1969).

The algorithm to derive vertical canopy profile metrics from waveform lidar is well developed (Armston et al., 2013a; Ni-Meister et al., 2010a, 2010b; Tang et al., 2012) and requires estimates of the following parameters to compute: (i) the integrated laser energy returns from the canopy  $R_v(z)$  and ground  $R_g$ ; (ii) the ratio of canopy and ground reflectance  $\rho_v/\rho_g$ ; (iii) the leaf area angle projection coefficient,  $G(\theta)$ , representing the fraction of canopy element area projected perpendicular to the view direction to the total canopy element area; and (iv) the clumping index,  $\Omega(\theta)$ , describing the spatial distribution pattern of canopy elements.

Here we set  $G = 0.5$  for a uniform random foliage distribution and  $\Omega = 1$ , which assumes that elements are dispersed randomly and independently between canopy layers. These assumptions are consistent with findings by Marselis et al. (2018) who validated the vertical profile metric estimates using independently acquired Terrestrial Laser Scanning (TLS) estimates. The  $R_v(z)$  and ground  $R_g$  are derived from LVIS level 1B and level 2 products by fitting an exponential Gaussian to the lowest waveform mode corresponding to the ground (Dubayah et al., 2020). The vegetation to ground reflectance ratio,  $\rho_v/\rho_g$ , is then set as a constant value per site (e.g. 1.493 for Mondah) using the method developed in previous studies (Armston et al., 2013b; Tang and Dubayah, 2017).

**LVIS gridded canopy cover and vertical profile metrics** were produced for the Lopé, Mondah/Akanda, Pongara, Rabi and Mabounié flightlines. The gridded map products were generated at 25 m (0.0625 ha) spatial resolution from footprint canopy cover metrics and profile data. The canopy cover and vertical profile metric grids generated include the mean and standard deviation of total canopy cover, foliage height diversity, total plant area index (PAI), and PAI in height intervals of 0–10 m, 10–20 m, 20–30 m, and 30+ m. Data product format, projection, and grid alignment were same as used for the LVIS gridded height models and bare earth DEMs.

**UAVSAR Tomographic SAR** products enable the generation of a wall-to-wall 3-dimensional map of vegetation structure (see Hawkins et al., 2018; Lavalle et al., 2016; Riel et al., 2018). Generally, a TomoSAR product describes the radar backscatter as a function of vertical elevation within the forest canopy and is thus related to the vertical distribution of material within the canopy (i.e. trunks, branches, leaves). Unlike Lidar, which results from intercepted surfaces, including leaves, L-band radar tomography penetrates deep into the canopy with greater sensitivity to large branches and trunks. The vertical resolution is driven by the length of the longest interferometric baselines in the tomographic stack and is therefore coarser than in the lidar data (ie m resolution in TomoSAR vs mm to cm in Lidar). The spacing between the interferometric baselines determines the height of ambiguity, which was set to be greater than the expected height of the forest. The three dimensional focusing of an image stack requires that each image has a common phase reference, which is especially difficult in the airborne case, since errors in the knowledge of the platform position are typically a large fraction of the size of the radar wavelength. For phase calibration, we adopted the approach described in Tebaldini et al. (2016) and Hawkins et al. (2018) where the full network of interferograms is reduced to a smaller set of “linked phases” and used to estimate a set of trajectory corrections having a consistent phase reference. The AfriSAR team generated two variants of the demonstrative Tomographic SAR products described below.

**UAVSAR TomoSAR:** products have backscatter values at several vertical height slices that can be used to generate canopy profiles and 3D canopy structure across the entire vegetation volume. These products were generated over Rabi and Lopé National Park as these were suitable for processing using tomographic imaging techniques described by



Hawkins et al. (2018), Lavalley et al., 2016). In these two sites, several flight lines ( $N = 8$ ) were acquired with different vertical baselines (i.e. separation between flights), spanning a vertical aperture of 120 m (see Table 3). Each flight line captures the radar backscatter projected onto its imaging plane and by varying the radar altitude between image acquisitions, we vary the angle of this projection and can therefore reconstruct the full backscattering profile. The tomographic processing begins with the single look complex (SLC) data products generated by the standard UAVSAR stack processor (see Table 3), which includes a motion measurement error calibration step (Hensley et al. 2015). To further reduce relative phase errors between the images in a stack, a second motion measurement error calibration step is performed (Tebaldini et al., 2016). Finally, the phase calibrated SLC images are considered samples of the backscatter vertical wavenumber spectrum, allowing the profiles to be recovered with spectral estimation techniques, either the discrete time Fourier transform (Reigber and Moreira, 2000) or the Capon method (Lombardini and Reigber, 2003). This results in a three-dimensional grid of radar backscatter throughout the vegetation volume and is therefore related to the vertical distribution of AGBD.

**UAVSAR TomoPLANT** products were generated for Mondah, Lopé National Park and Rabi, starting from the stack of polarimetric SLC images using a processing chain based on ISCE and PLANT tools (Lavalley et al., 2018). Polarimetric Coherence TomoSAR (PCT) forest structure products were derived by expanding a second order Legendre polynomial expansion (Cloude, 2006) between the ground and the estimated tree height, in this case the lidar-based canopy height, to generate the forest vertical backscatter profile. Similar to the above method, the vertical wavenumber layers and phase-calibrated tomographic SLC images were then used to estimate the vertical reflectivity for each polarimetric channel using the standard Capon and Fourier beamforming. The generation of polarimetric coherence TomoSAR profiles also required the use of the tree height product generated using PolInSAR technique.

#### 4.5. AfriSAR Biomass Products

**LVIS gridded Aboveground Biomass Density and associated error:** AGBD was estimated for Lopé, Mondah, Rabi and Mabounié using a model that follows the functional form of the scaling equations used to derive mass from individual tree structure:

$$AGBD \text{ (Mg ha}^{-1}\text{)} = H^a \cdot BAD^b \cdot WSG^c \quad (1)$$

where  $H$  is the canopy top height,  $BAD$  is basal area density and  $WSG$  is the wood specific gravity. This model form has been widely used in the literature, for example Asner et al. (2011) to estimate AGBD in the tropical forests of Central and South America, Madagascar, and the Island of Hawaii. We used RH98 for the Canopy top height ( $H$ ) since this is less sensitive to noise (Hancock et al., 2019). However, this model is also parameterized in terms of basal area density ( $BAD$ ) and wood specific gravity ( $WSG$ ), neither of which are directly measured by the lidar waveforms. Therefore, to model  $BAD$  in this study, we developed a linear model parameterized by canopy cover ( $CC$ ) and height ( $z$ ), as previously shown by Asner and Mascaro (2014) and Ni-Meister et al. (2010a, 2010b), for predicting  $BAD$  from lidar measurements:

$$BAD \text{ (m}^2 \text{ ha}^{-1}\text{)} = RH90 \cdot CC_{z=H_{max}} \quad (2)$$

where  $CC_{z=H_{max}}$  is canopy cover at the top of canopy (i.e. total cover).

The AGBD model was developed using field measurements from Mondah, Lopé, and Mabounié. Models were independently developed at spatial resolutions of 50 m (0.25 ha) and 100 m (1 ha), for which we had in situ estimates of AGBD that could be co-located with waveform footprints with relative geolocation errors of <5%. Specification of these models required explicit treatment of heteroscedasticity and the non-

normal error distribution of the response (AGBD). To address this requirement, we used a Generalized Linear Model (GLM), selecting a Gamma distribution for modelling the continuous, non-negative and positive-skewed AGBD data. The variance of the Gamma distribution is proportional to the squared means, thus allowing this form of heteroscedasticity to be specified and avoiding the assumption of homoscedasticity. An identity link function was used, since we observed AGBD was linearly related to the non-linear combination of predictors in Eq. 1. Estimation of the model parameters was undertaken in a Bayesian framework using the R package 'brms' (Bürkner, 2017). Posterior predictive distributions provided realistic per-pixel estimates of uncertainty in the form of 95% confidence intervals. Model performance was assessed by leave-one-out (LOO) cross-validation.

#### 4.6. Dataset intercomparison

We compared the accuracies and sensitivities of the height and AGBD products by extracting the values of the RH100,  $CHM_{PLANT}$ ,  $CHM_{KAPOK}$ ,  $CHM_{FUSION}$  data (for height) and  $AGBD_{LVIS}$ , with the small footprint lidar datasets by Labriere et al. (2018) and plotting them against each other. To achieve this, we extracted all points covering the overlapping areas between LVIS and the radar products. The values of each point were then plotted and basic statistics calculated ( $r^2$ , intercept, slope, RMSE, residual error,  $p$ -value). Crossovers between LVIS and discrete return ALS data were used for comparison of equivalent products for each dataset at the Lopé, Mondah/Akanda, Rabi and Mabounié sites. To ensure both datasets were aligned, horizontal offsets were calculated by maximizing the correlation between real and ALS simulated LVIS waveforms (Blair and Hofton, 1999; Hancock et al., 2019) and then applied.

For the TomoSAR analysis, lidar waveforms were reprojected to the radar geometry to ease the comparison with tomograms. Furthermore, radar tomograms have been normalized to their maximum vertical value to highlight the vertical structural changes and to avoid that a bright concentrated target shadows scattering elements less bright but more distributed along elevation.

### 5. Data product analysis

Here we present the analysis of the level 3 data products. These data products are accessible through the NASA Earthdata Search Portal for AfriSAR at <https://search.earthdata.nasa.gov/search?q=afrisar> and the Oak Ridge National Laboratories Distributed Active Archive Center for Biogeochemical Dynamics at <https://daac.ornl.gov/>.

#### 5.1. In situ aboveground biomass density

We measured 6692 trees from 139 species in Mondah, with DBH values ranging from 5 cm to 198.4 cm and maximum measured heights of 59.23 m. Mean AGBD was 103.2 Mg ha<sup>-1</sup> and ranged from 3.26 Mg ha<sup>-1</sup> to 267.5 Mg ha<sup>-1</sup>. All vegetation characteristics and estimates of AGBD were reported at multiple scales: 0.0625 ha, 0.25 ha, and 1 ha. These data are available on the ORNL DAAC (Fatoyinbo et al., 2018) and were used to validate and calibrate the NASA AfriSAR higher level data products described below.

#### 5.2. LVIS footprint level canopy cover metrics and profiles

Canopy cover and height distribution across plots varied greatly, highlighting the difference in stand structures across sites. Examples of canopy metric data products over the Mondah flight lines are shown in Fig. 2. All LVIS based data products are shown in Fig. 3. Taller stands, as shown in plot NASA 13, Fig. 2 with a 40+ m canopy had lower plant volume throughout the vertical canopy profile, with the highest density in the understory, while the medium stature (~25 m canopy) plot NASA 21A's plant area was dense throughout the entire canopy layer. Plot 20 on the other hand had a similar canopy height to plot 21, but lower

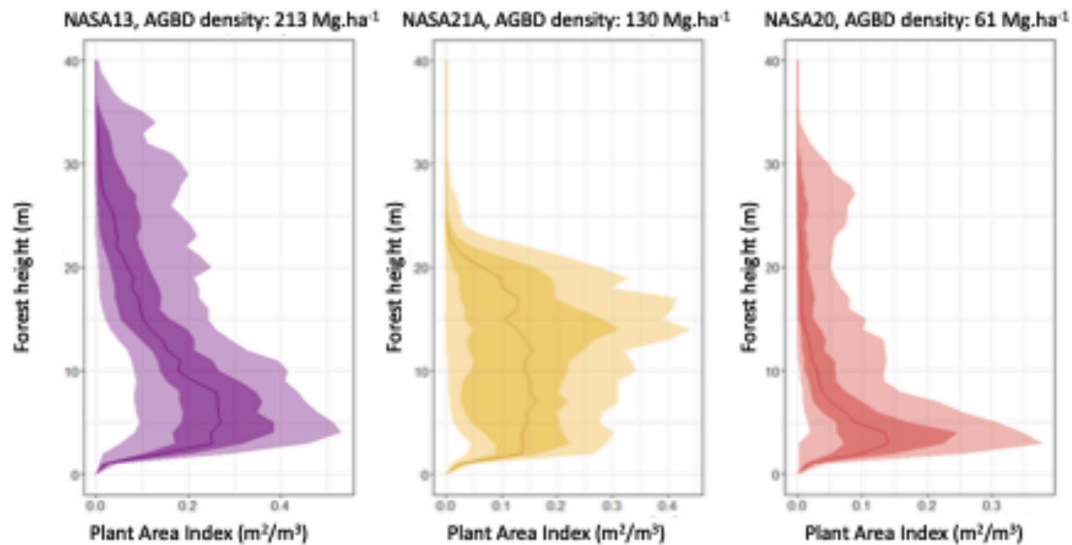


**Fig. 2.** Plant area volume density as a function of canopy height in three plots in Mondah forest (plot 13, 21 and 20). The lightest shade is 0.1–0.9 percentile, the darker shade is 0.3–0.7 percentile and the line is the 0.5 quantile.

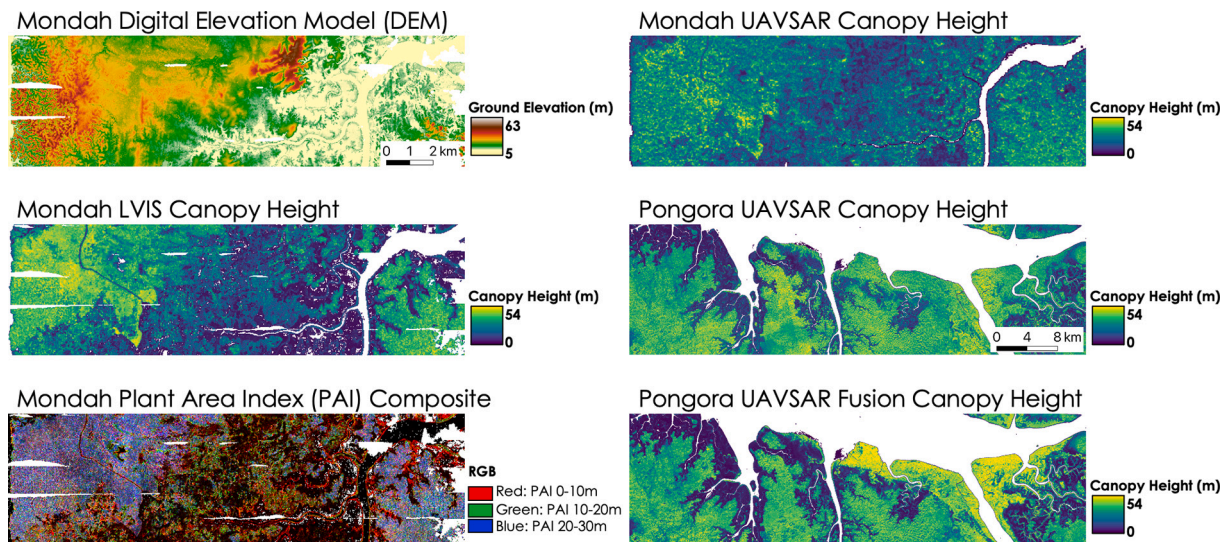


**Fig. 3.** LVIS and UAVSAR gridded data products for Mondah and Pongora at 30 m resolution. In the left pane, the following gridded metrics are shown from top to bottom: Gridded Digital Elevation Model for Mondah, RH100 for Mondah, Plant area index composite of 0 m–10 m (red), 10 m–20 m (green), 20 m–30 m (blue) plant area index between 0 and 10 m vertical, plant area index between 20 and 30 m vertical and canopy cover fraction. In the right pane, the following gridded products are shown from top to bottom: CHM<sub>Kapok</sub> Canopy Height, CHM<sub>Kapok</sub> Canopy height for Pongora, CHM<sub>Fusion</sub> Canopy height for Pongora. (For interpretation of the references to colour in this figure legend, the reader is referred to the web version of this article.)

AGBD and a majority of the plant area volume concentrated in the lowest 5 m of the canopy, suggesting a difference in forest composition and/or forest management strategy between the 3 plots.

In the comparison of the LVIS and ALS crossovers of the canopy metric products, there was a mean negative bias (LVIS cover estimates are lower than ALS) of between 5.9% at Mabounie and 11.2% at Mondah with the corresponding RMSE between 15.5% and 24.2%. Mondah was not included in these statistics because of the 5 years between the ALS and LVIS acquisition dates and large areas of secondary forest growth. The differences in cover estimates between LVIS and ALS are in some cases the result of errors in ground return energy estimates. It is important to note that ALS does not provide a direct estimate of canopy cover, which can cause systematic differences (see [Armston et al., 2013a](#); [Fisher et al., 2020](#)), but this small negative bias in LVIS estimated canopy cover is consistent with what we would expect from the small positive bias in LVIS estimated ground elevation (0.6–2.3 m across all

sites) described below.

### 5.3. LVIS footprint level height and elevation metrics

LVIS to ALS footprint cross-over comparisons showed the RMSE for ground elevation ranged between 1.75 m for Mondah and 4.2 m for Lopé. The mean bias was positive (LVIS elevation estimates above ALS estimates) and ranged between 0.64 m for Lopé and 2.3 m for Rabi. There was a weak trend of increasing positive mean bias (LVIS elevation estimates above ALS estimates) and RMSE with increasing canopy cover and slope. Uncertainties in subcanopy ground elevation estimates from large-footprint waveform lidar have been well explained in the literature (Hofman et al. 2000, Duncanson et al. 2010, Hancock et al. 2012). In the case of mangroves, underlying conditions such as the presence of water (tides) or aboveground roots (such as mangrove prop roots) may also affect the ability of the LVIS algorithm to accurately estimate the

elevation of the ground.

#### 5.4. LVIS gridded height models and bare earth DEMs

The largest height metrics were found in Lopé National Park, with maximum canopy height estimates in the gridded LVIS product of 84.3 m for RH100 and 75.9 m using RH98. At the individual footprint level, the maximum heights at Lopé are 93.5 m for RH100 and 88.9 m for RH98, highlighting the impact of spatial averaging to 25 m on gridded height estimates. Over areas with complex topography (e.g. gullies), such as Lopé, the ground waveforms at the spatial resolution of LVIS or GEDI footprints can be multi-modal, meaning that the lowest mode may not always be the only ground return, thereby resulting in RH metrics being larger than actual individual tree height. Maximum gridded height values are 64.2 m (55.17 for RH98) in Mondah, 65.1 m (51.5 m for RH98) for Pongara, 76.6 (49.4 m for RH98) for Rabi, 75.26 m (50.3 m for RH98) in Mabounié.

The bare earth gridded DEM height is presented as height over the geoid, and ranges from the lowest areas of 8 m in Pongara to 671 m in Lopé National Park, highlighting the wide range in topography and environmental settings covered. Overall, the subcanopy bare earth height range for Lopé is from 101 m to 671.8 m, from 10 m to 63.3 m in Mondah, from 10 m to 243.2 m in Rabi, and from 8.9 m to 138.8 m in Pongara.

#### 5.5. LVIS gridded Aboveground Biomass density and associated error

For the 3 sites, mean AGBD ranged from 337 Mg ha<sup>-1</sup> +/− 165 Mg ha<sup>-1</sup> in Lopé National Park to 249 Mg ha<sup>-1</sup> +/− 145 Mg ha<sup>-1</sup> in Mabounié and 86 Mg ha<sup>-1</sup> +/− 138 Mg ha<sup>-1</sup> in Mondah forest. The calibration results for the LVIS AGBD estimators at 1 ha and 0.25 ha spatial resolution using Mondah, Lopé and Mabounié plot data is shown in Table 4. Estimator parameters were not significantly different at 0.25 and 1 ha spatial resolutions, with greatest uncertainty in the stand wood density (SWD) parameter. Estimator performance was best at the 1 ha resolution, with an  $r^2$  of 0.82 and RMSE of 85 Mg ha<sup>-1</sup>, whereas the 0.25 ha resolution model had an  $r^2$  of 0.72 and RMSE of 114 Mg ha<sup>-1</sup>.

In the comparison of AGBD<sub>LVIS</sub> vs ALS-based AGBD data (Fig. 4), the LVIS-based AGBD estimates were close to the AGBD<sub>Labriere</sub>, with  $r^2$  of 0.86, RMSE of 25% and a bias of 6%. The differences in AGBD derived from ALS and LVIS can be attributed to multiple reasons – temporal differences, particularly secondary forest growth in Mondah Forest between the 2012 ALS and the 2016 LVIS Lidar acquisitions in addition to differences in sampling error (number of LVIS shots per grid cell) between grid cells.

#### 5.6. UAVSAR canopy height

UAVSAR height product accuracies were assessed through a regression with LVIS RH100 metrics. Comparisons of the three UAVSAR canopy height products with LVIS are shown in Fig. 3 and Fig. 5.

The UAVSAR Canopy height models performed better in Pongara than in Lopé, likely due to the flat topography of mangrove forest of Pongara. The Lopé and Mondah sites are characterized by large

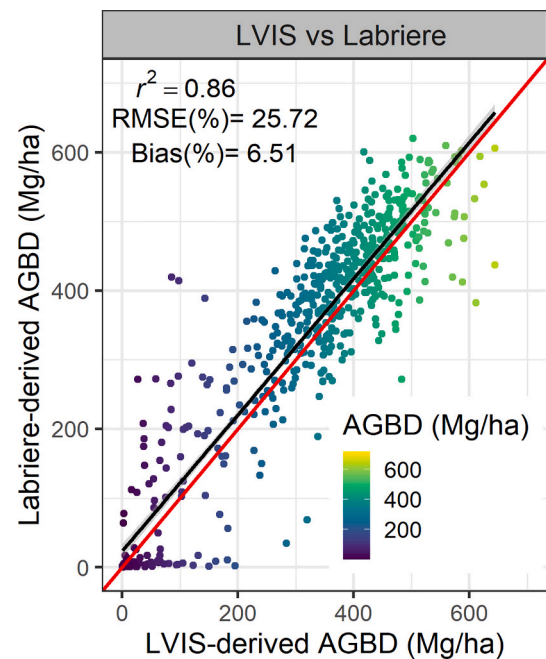


Fig. 4. Comparison of airborne lidar-derived AGBD estimates (Labriere et al. 2018 and Armston et al., 2020) in Lopé National Park.

topographic gradients and many areas of steep slopes. The UAVSAR's CHM<sub>Fusion</sub> canopy height product is the most accurate, as compared to LVIS RH100, with the highest  $r^2$  (0.84 in Pongara and 0.74 in Lopé), lowest RMSE (around 27%) and low bias (3.65% for Pongara). Good agreement between these datasets is expected as the CHM<sub>Fusion</sub> product used a sparse subset of LVIS RH100 data to train the classifier.

The CHM<sub>Fusion</sub> model overestimates canopy height in short mangroves, most likely due to the impact of temporal decorrelation being more significant relative to volume decorrelation. Changes in water level that occur in these open and short stature mangrove forests between UAVSAR acquisitions may also have a greater impact on radar signal. CHM<sub>Kapok</sub> also overestimated shorter trees and underestimated taller canopies when compared to RHh100 with  $r^2$  of 0.73 and 0.63 in Pongara and Lopé respectively and RMSE of about 33%. Similarly to the CHM<sub>Fusion</sub>, the CHM<sub>Kapok</sub> product was biased, with mangrove heights (in Pongara) being generally overestimated (bias of 7.23%) and tall trees of Lopé underestimated with an overall bias of −9.94%. Similarly to CHM<sub>Kapok</sub>, CHM<sub>PLANT</sub> generally underestimated tall trees while overestimating short ones when compared to RHh100. The comparison resulted in  $r^2$  values of 0.76 for Lopé, 0.54 for Mondah and 0.24 for Rabi, and biases ranging from 14.48% in Mondah to −32.9% in Rabi (Fig. 5).

These comparisons highlight that the deviation between UAVSAR- and LVIS-derived canopy maps depends significantly on the choice of the interferometric baseline, forest structure, presence of temporal decorrelation, terrain conditions, and the inversion model. Generally speaking, UAVSAR canopy height estimates are most accurate over a

Table 4

LVIS AGBD model performance at 1 ha and 0.25 ha spatial resolution using Mondah, Lopé and Mabounié plot data. Parameter estimates and model fit statistics were estimated using leave-one-out cross validation.

Resolution	R <sup>2</sup>	RMSE	Parameter	Estimate	Error	Lower 95% CI	Upper 95% CI
1 ha	0.82 (0.04)*	84.94	SWD	−1.84	0.68	−3.17	−0.51
			RH98	0.01	0.15	−0.30	0.30
			SBA	0.24	0.07	0.11	0.38
0.25 ha	0.72 (0.01)	114.07	SWD	−1.86	0.43	−2.70	−1.00
			RH98	−0.02	0.10	−0.20	0.17
			SBA	0.27	0.04	0.19	0.35

\* where SWD is stand wood density, WD is Wood Density and SBA is stand Basal Area.



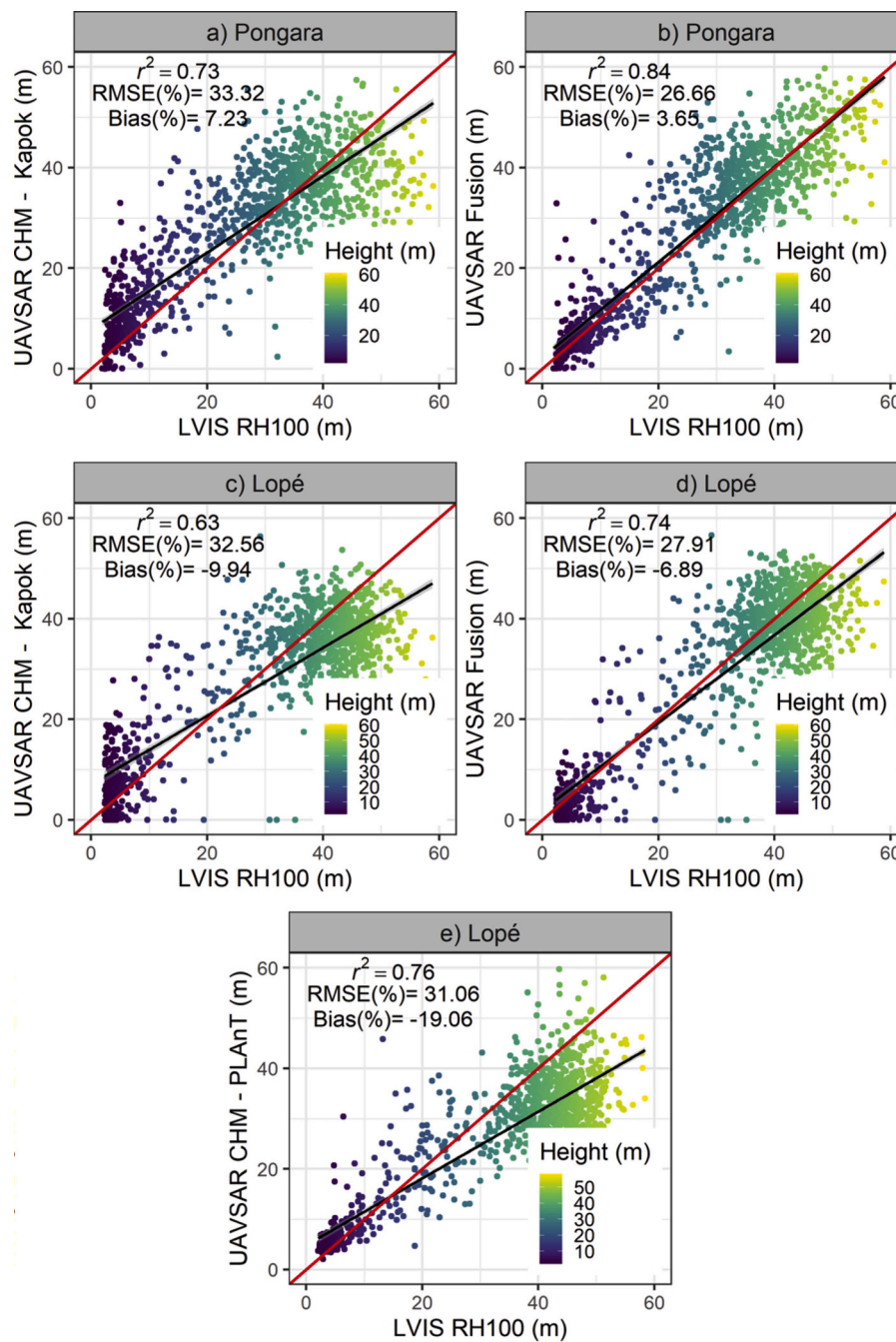


**Fig. 5.** Comparison of LVIS Rh 100 standard height products with 3 UAVSAR Pol-InSAR height products CHM Kapok (Denbina et al, 2018), CHM Fusion (Denbina et al, 2018) and CHM Plant (Lavalley et al., 2018).

height range between 10 and 30 m due to L-band penetration in the canopy and the implementation of the UAVSAR repeat-pass interferometric flights. The quality of the height retrieval degrades as the retrieved height approaches values lower than 5 m, which may be dominated by temporal decorrelation, resulting in an overestimation of short heights. For values greater than 40 m, the effects of the microwave penetration and saturation of the L-band signal may lead to an underestimation of maximum (RH100) tree height.

### 5.7. UAVSAR Tomographic SAR

We generated SAR tomograms using the Capon, Fourier and Polarization Coherence Tomography techniques, as shown in Fig. 6. The

transects is 1.7 km long and 20 m wide where topography varies by about 50 m and land cover ranges from bare soil or short vegetation to 40 m tall trees. Generally, the radar tomograms and lidar waveforms agree with each other, especially over short vegetation. In these regions, mainly concentrated in the horizontal intervals 0–300 m and 550–800 m in Fig. 6, the lidar height metrics, along with the Capon and the PCT tomograms show similar patterns of vertical volume distribution across the transect, suggesting that these tomographic techniques are good candidates for estimating vegetation structure patterns. Over tall trees in the intervals 300–550 m and beyond 800 m, all SAR-based transect show modulations of vertical brightness depending on the vegetation structure and underlying soil scattering that need to be taken into account.

The tomogram resulting from the Fourier technique has a coarse

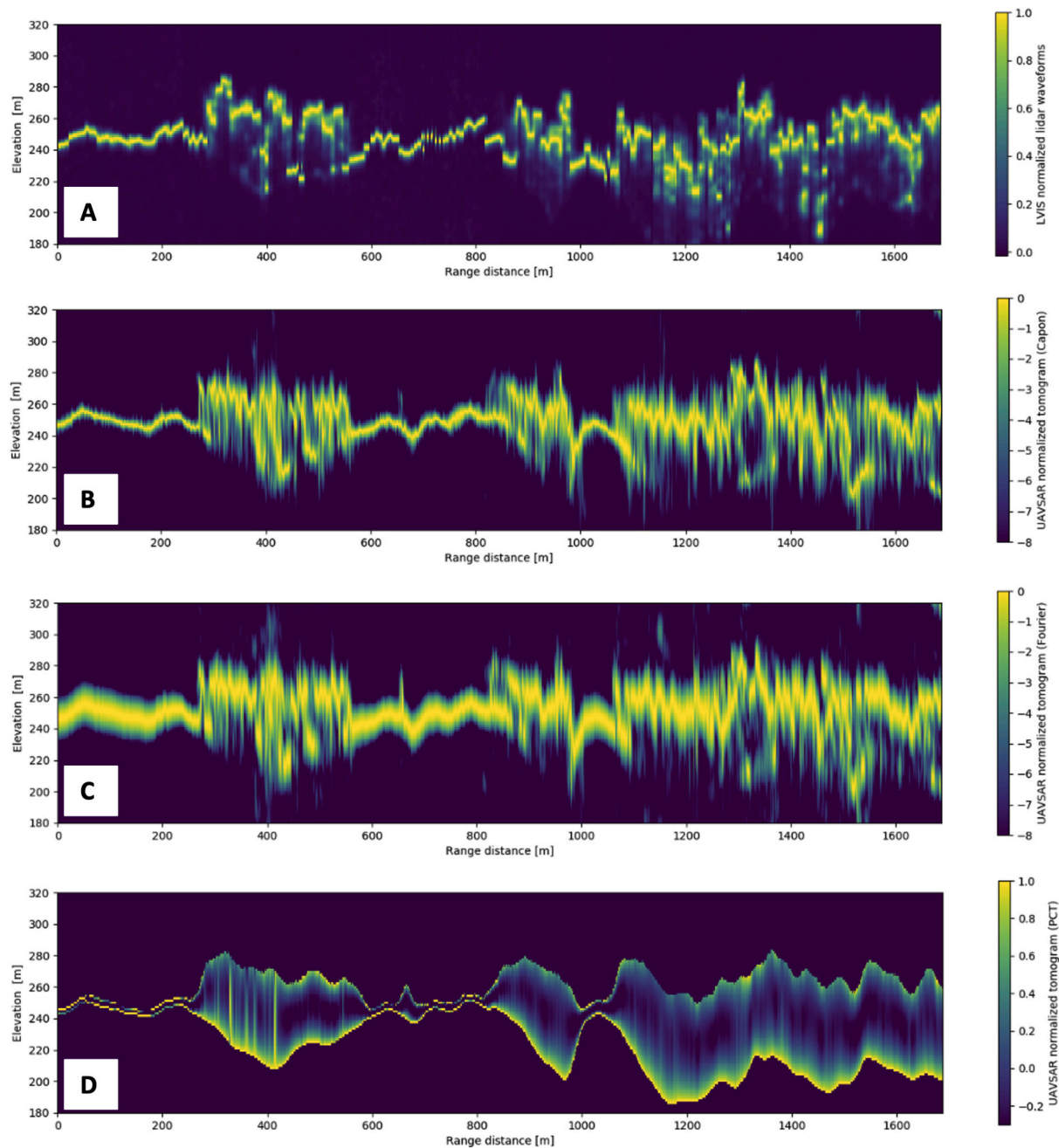


**Fig. 6.** Comparison of transects of LVIS (A) with TomoSAR Fourier (B), PCT (C) and Capon (D) data projected into radar geometry in the Lope National Park site. The color scale ranges from dark blue (low values) to yellow (high values) and indicates the normalized waveform return (panel A) and the normalized radar HV backscatter (panels B, C and D). (For interpretation of the references to colour in this figure legend, the reader is referred to the web version of this article.)

vertical resolution of about 8 m as highlighted of over bare earth or short-vegetated areas and is therefore less suitable for fine vertical resolution mapping of tree canopies. As expected, the Fourier tomogram also has larger side lobes compared to the Capon and PCT tomograms, with the canopy reflectivity “leaking” above the expected tree height, giving the profile a blurrier appearance.

The exact features of TomoSAR measurements are more visible when vertical profiles of the four techniques are extracted from an approximately 20 m by 20 m square column or equivalent LVIS footprint as shown in Fig. 7. Here, the profiles have been normalized to their maximum value along the vertical direction, with all peaks equal to 1. Most notably, the profiles have multiple peaks, one strong peak representing the ground and another weaker but wider peak about 20 m above the ground representing the bulk of the canopy returns. The

Capon and Fourier tomograms are in good agreement with the corresponding LVIS profiles with profiles produced using the Capon algorithm most similar to the LVIS profile, although tomographic profiles change with the polarimetric channels (Fig. 7) revealing different scattering mechanisms within the canopy and in the ground-trunk scattering interaction. Note that, from Fig. 7, canopy height could be estimated from the UAVSAR TomoSAR products as the maximum vertical extent of the tomograms, although additional corrections would be required to account for L-band penetration, look angle, resolution and overall sensitivity (Shiroma and Laval, 2020). More specifically, the differences in viewing geometry between the nadir looking lidar and the side looking TomoSAR profiles, and different interactions with canopy components may result in different parts of the canopy being represented. Here our results show that lidar waveforms and L-band radar

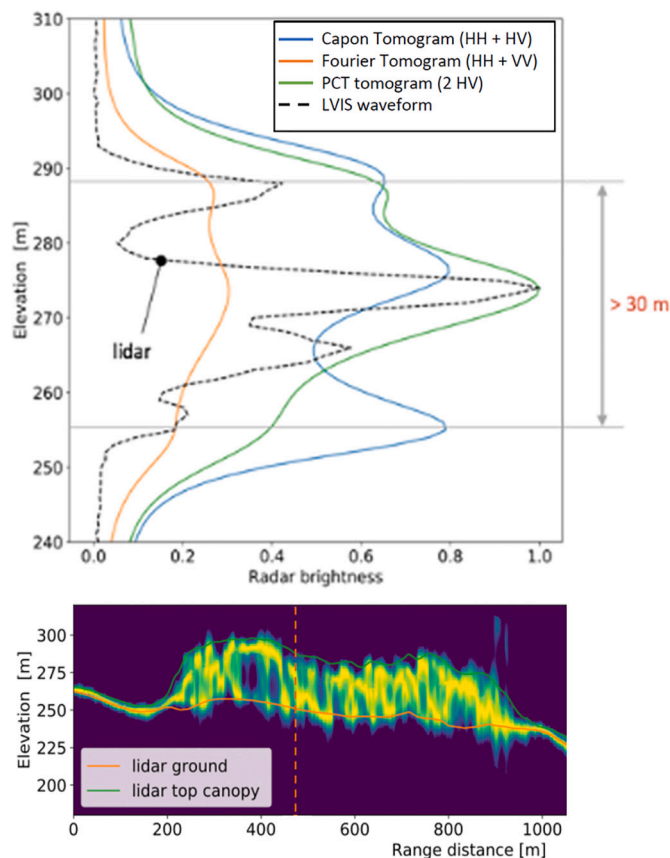


Fig. 7. Comparison of TomoSAR Capon, Fourier, PCT data overlaid on a LVIS waveform projected into radar geometry in Lope National Park for a 20 m by 20 m area.

tomograms have similar overall responses over forest canopies even though they are based on measurements at different wavelength and thus different scattering mechanisms. More detailed analyses of SAR tomograms collected as part of AfriSAR and their implications for forest vertical structure measurements can be found in Shiroma and Laval, (2020) and Pardini et al. (2019).

The tomographic SAR profiles produced using the Capon technique are most similar to the LVIS profile, although large differences between the retrievals of each polarization are still present. The estimated Capon and Fourier ground location are in good agreement with LVIS, although the ground detected by UAVSAR here is generally higher than what was measured by LVIS. The estimated maximum canopy height from the UAVSAR TomoSAR product is comparable to canopy height from LVIS, although there is still some error due to L-band penetration, look angle, resolution and sensitivity. More specifically, there are significant geometric differences between lidar waveforms and the TomoSAR profiles leading to differences between measurements, such as LVIS being nadir looking whereas TomoSAR is side looking and then projected onto a vertical height axis.

## 6. Discussion

The 2016 NASA AfriSAR mission was the first simultaneous acquisition of polarimetric SAR, waveform lidar and field data in support of the upcoming NISAR, GEDI and Biomass missions and the first coordinated campaign for measurements of forest structure properties across multiple international space agencies. While similar campaigns flying LVIS and UAVSAR have been carried out, such as the 2009 and 2010 DesdynI Cal/Val campaigns in Howland, Harvard and Penobscot Experimental Forests (Montesano et al., 2013), the amount of data

collected and area covered was much lower than accomplished by AfriSAR. Furthermore, previous campaigns did not include multiple baseline or tomographic SAR acquisitions. Here, we collected over 7000 km<sup>2</sup> of Lidar and 30,000 km<sup>2</sup> of PolSAR data, covering 30% of the Gabonese territory and all of the major terrestrial ecosystems of Central African Region.

The AfriSAR data have been key in advancing forest structure retrieval algorithms, image processing software, spaceborne data simulation and biodiversity mapping methodologies amongst others. In Denbina et al. (2018b), the new Kapok software package to generate canopy height from repeat-pass UAVSAR data was developed using UAVSAR and LVIS airborne acquisitions over Pongara and Lope National Parks, while the ISCE-PLANT software was developed over Lope, Mondah and Rabi sites. Similarly, this dataset was instrumental in developing new machine learning approaches to fuse SAR and Lidar data (Denbina et al., 2018b, (Pourshamsi et al., 2018). Here the subsampled LVIS data was used to select the best baseline configuration and  $k_z$  value, i.e. to determine whether a large or shorter baseline configuration between two UAVSAR acquisitions should be used in multiple baseline PolInSAR processing.

On the Lidar side, the AfriSAR data was one of the key datasets used for validation of the GEDI-simulator (Hancock et al., 2019a), pre-launch calibration and validation of GEDI Level 2 footprint product algorithms (Hofton and Blair, 2019; Tang and Armston, 2019), and is an ongoing key component of GEDI's post-launch calibration and performance assessment strategy (Dubayah et al., 2020). It has also been used in combination with other SAR datasets, such as Sentinel-1, to generate country wide (Lang et al., 2019) and site-wide (Pourshamsi et al., 2018) canopy height and AGBD (Marshak et al., 2020) estimates.

Areas of dense canopy cover as found in Gabon may sometimes present a challenge for lidar measurements, particularly over complex topography. LVIS was designed to be sensitive enough to detect a ground pulse in canopy cover of up to 99% and comparisons with small-footprint systems have shown this to be true (Hofton et al., 2002). However, certain environmental conditions such as steep slopes or low-lying canopy material such as shrubs can weaken already weak ground returns to the point where automated ground finding algorithms misidentify the ground. Here, LVIS was deployed over the most challenging forest conditions - the combination of high canopy cover, wide ranges of topographic relief and different types of forest types and densities. Despite these conditions we showed a high degree of consistency in estimating canopy structure parameters from airborne waveform lidar data. We also found excellent agreements with PAI profiles derived from terrestrial laser scanner (TLS) even at a high vertical resolution (1 m) (Marselis et al., 2018). In sum, our results highlight the fidelity of LVIS-based vegetation structure products and strengthens the confidence in our data processing algorithms.

The extensive UAVSAR collection over a wide range of forest types and biomass added important new sites for the NISAR mission calibration and algorithm development, with the addition of 15 new 1-ha plots in lower biomass areas and extensive airborne Lidar data needed for AGBD calibration and validation. Indeed, while a breadth of field measurements was previously available in Central African forests, 90% of all plots were in high biomass forests (over 200 Mg/ha). Through the additional field data collected here we have expanded the range in AGBD measurements available for the tropics with plot AGBD densities ranging from 50 to 250 Mg/ha. In the case of UAVSAR, this was the first extensive PolInSAR and tomographic experiment over tropical forests. While TomoSAR and PolInSAR processing have been carried out before with UAVSAR (Hensley et al. 2015), the AfriSAR campaign allowed for extensive experiments on baseline and temporal decorrelation. Here, we were able to generate canopy height products using multiple methodologies, using the PLANT software (Laval et al., 2018b), the Kapok software and the Fusion approach (Denbina et al., 2018a) which helped determine the limitations and strengths of each methodology and the ideal configurations for L-band multibaseline PolInSAR acquisitions in



dense tropical forests.

As an example, the fact that the ‘fusion’ approach performs better at estimating the RH100 or Top of Canopy height than the traditional PolInSAR approaches highlights the potential improvement when using SAR-Lidar fusion or other ancillary data that helps in selecting the appropriate interferometric baseline. The lower bias between the CHM<sub>Fusion</sub> products and the more traditional PolInSAR methodology highlights the importance of selecting the appropriate baseline, especially in areas like Gabon, where the range in heights is high (up to 65 + m).

The demonstration of the Tomographic SAR capabilities in tropical forests of Gabon served to develop and evaluate several algorithms that will be used to improve the design of future airborne experiments and spaceborne missions. Similar to [Pardini et al. \(2019\)](#), the Lidar profiles are more sensitive than TomoSAR reflectivity profiles to variations in the top of the canopy, however, TomoSAR long-wavelength profiles (from L- and P-band) are more sensitive to below-canopy variations in vertical structure. Thus, in addition to providing structural information complementary to Lidar, TomoSAR could effectively improve carbon stock estimates and sensitivity to forest disturbances. Importantly, TomoSAR may enable the generation of wall-to-wall maps of vertical distribution of material within forest canopies due to its all-weather capability. Finally, while the operational repeat-pass mode of the NISAR mission does not allow for TomoSAR or multi-baseline PolInSAR acquisitions, the multi-baseline acquisitions of the ESA BIOMASS mission will provide the necessary datasets.

The released UAVSAR and LVIS datasets provide a large quantity of coincident (PolIn)SAR and lidar coverage, ideal for the development and testing of algorithms which fuse the results from these sensors. While SAR data has wide spatial coverage and high resolution, it can be affected by some limitations and error sources such as temporal decorrelation and saturation in high AGBD forests. Lidar can generally estimate forest canopy height and vertical variations in canopy structure with high accuracy but is limited in terms of spatial coverage. Fusion algorithms can therefore help to mitigate the weaknesses of each sensor, combining the data into fused products which leverage the strengths of both lidar and SAR. The released CHM<sub>Fusion</sub> fused canopy height and AGBD products help demonstrate examples of this potential, and the released L1 UAVSAR and LVIS data can be used for development and testing of other future algorithms, which can be applied to spaceborne data from GEDI, NISAR, Biomass, and other future sensors.

One of the main hurdles for the uptake and use of lidar and SAR by the broader ecological and scientific community has been the lack of gridded and higher level products available from waveform Lidar and SAR data. Data from sensors with existing and well documented ARD products have much higher use than sensors without, highlighting the importance of providing not only raw data but also preprocessed datasets. As an example, the SRTM DEM, a processed and tiled product derived from C-band single pass interferometry, is one of NASA’s most downloaded datasets, although it is only based on a one-time acquisition in early 2000 ([Farr et al., 2007](#)).

As part of the AfriSAR campaign, we have produced a suite of data products from UAVSAR and LVIS that have not been available to date, such as LVIS-derived canopy cover fraction, Plant Area Index, Gridded canopy height from LVIS and UAVSAR Pol-InSAR and Tomographic SAR products, allowing the development of new scientific applications. In [Marselis et al. \(2018\)](#), for example, the LVIS canopy cover profile data products were used to predict successional vegetation types in Lopé National Park, with potential implications for the use of GEDI data for informing conservation and biodiversity studies. The dataset was also key in the development of a methodology to map tree species diversity using canopy structure data ([Marselis et al., 2019](#)) using GEDI-like data. We anticipate and encourage a wide range of future applications, such as the development of new algorithms that make use of the SAR SLC stacks and associated geometric parameters (e.g. [Soja et al., 2021](#)). The unique combination of multi-modal remote sensing and field datasets produced

by AfriSAR are also the basis of the Biomass Retrieval Inter-comparison eXperiment (BRIX-1 and BRIX-2), which will benchmark biomass retrieval algorithms using GEDI, NISAR and ESA BIOMASS data on the joint ESA-NASA Multi-mission Analysis and Algorithm Platform (MAAP; [Albinet et al., 2019](#)).

AfriSAR was an experimental campaign for which several new SAR and Lidar algorithms were developed and implemented. Because of the limitations that arise during airborne experiments, such as time constraints and changes in flying conditions, there were flight configurations and data acquisitions that resulted in data that did not capture the entire range of forest structure conditions. An example is the vertical wavenumber configuration of the SAR experiments limiting the acquisition of the full height range in all of the imaged sites, or the presence of clouds and poor conditions in some LVIS acquisitions leading to gaps in the data. In addition, while the NASA AfriSAR campaign was designed to acquire data over as many forest ecosystem types as possible there is still a lack of data in certain key areas and types of measurements, such as flooded freshwater forests, wetlands or temporal forest structure changes. We therefore recommend follow-on airborne experiments focused on different types of ecosystems, including wetlands, dry forests, temperate forests as well as repeat measurements that allow the estimation of forest structure changes.

The AfriSAR campaign also provided the opportunity to advance applications of current airborne and future spaceborne missions in the field of tropical forest ecology, conservation and biodiversity. African rainforests in particular have suffered extensive clearing and fragmentation; it is estimated that West and Eastern Africa and Madagascar have lost about 90% of their original rainforest cover, whereas about 60% of the Central African forests still remain with much lower deforestation rates ([Malhi et al., 2013](#)). The Central African forest studied as part of AfriSAR is the second largest tropical forest after the Amazon, and better data, such as that expected from current and future missions, is crucial to better inform its management.

## 7. Conclusions

The airborne SAR, Lidar and field data acquired during the AfriSAR campaign constitutes a rich dataset for use not only in support of the NISAR, BIOMASS and GEDI missions, but also for improved understanding and monitoring of Central Africa’s tropical forests, wetlands and savannas. We anticipate that the dataset and described data products will be of use for studies of water and carbon cycling in the Congo basin, used as input and validation for forest growth models and to evaluate conservation and forest management practices. The high-resolution canopy height and vertical structure distribution data will be of direct use for studies of carbon cycling and biodiversity amongst many other applications.

Spatially explicit estimates of the vertical dimension of forests are needed to characterize rapidly changing global forest cover and AGBD, monitor disturbance, and assess biodiversity ([Bergen et al., 2009](#)). The suite of current and upcoming active Remote Sensing missions, including GEDI, BIOMASS, and NISAR, is expected to provide the global scale estimates of canopy height, vertical forest structure and forest density at the resolutions (1 km or better) and accuracies (20% error for 80% of the grid cells) needed to improve our understanding of the role of the land carbon sink in the global carbon cycle.

Combining multiple active datasets is already of immense interest, and this is only expected to increase with the impressive amount of data promised from GEDI, NISAR and BIOMASS. The AfriSAR datasets have allowed us a snapshot of the capability of not only the individual missions’ measurements, but also the exciting range of science and applications possible through Lidar and SAR data fusion.

## Declaration of Competing Interest

The authors declare that they have no known competing financial

interests or personal relationships that could have appeared to influence the work reported in this paper.

## Acknowledgements

The AfriSAR campaign and data product development was supported by NASA's Earth Science Division of the Science Mission Directorate. This work was funded by NASA's Terrestrial Ecology program, the Carbon Monitoring System grant (CMS, grant 15-CMS15-0055) and NASA's New Investigator Program (NIP, grant #80NSSC18K0708). This work was partly conducted by the Jet Propulsion Laboratory, California Institute of Technology, under contract with the National Aeronautics and Space Administration.

We would like to express our gratitude to the Gabonese Spatial Studies and Observation Agency (AGEOS, Agence Gabonaise de l'Etude et Observation Spatiale), the Gabon National Park Agency (ANPN, Agence Nationale des Parcs Nationaux), the Gabon National Scientific Research Center (CENAREST, Centre National de la Recherche Scientifique) and the Gabon-Oregon Center (GOC) for their invaluable collaboration and support of the AfriSAR airborne and field campaigns in Gabon. In particular, we would like to thank Bruno Stephane Dzime, Karl Igor Longa, Flore Kouamba, Francis Bivigou and the ANPN field teams. We would also like to thank our collaborators from ESA, DLR, ONERA and CNES for the invitation to participate in the campaign.

## Appendix A. Supplementary data

Supplementary data to this article can be found online at <https://doi.org/10.1016/j.rse.2021.112533>.

## References

- Albinet, C., Whitehurst, A.S., Jewell, L.A., Bugbee, K., Laur, H., Murphy, K.J., Frommknecht, B., Scipal, K., Costa, G., Jai, B., Ramachandran, R., Laval, M., Duncanson, L., 2019. A Joint ESA-NASA Multi-mission Algorithm and Analysis Platform (MAAP) for Biomass, NISAR, and GEDI. *Surv. Geophys.* 40, 1017–1027. <https://doi.org/10.1007/s10712-019-09541-z>.
- Armstrong, J., Disney, M., Lewis, P., Scarth, P., Phinn, S., Lucas, R., Bunting, P., Goodwin, N., 2013a. Direct retrieval of canopy gap probability using airborne waveform lidar. *Remote Sens. Environ.* 134, 24–38. <https://doi.org/10.1016/j.rse.2013.02.021>.
- Armstrong, J., Disney, M., Lewis, P., Scarth, P., Phinn, S., Lucas, R., Bunting, P., Goodwin, N., 2013b. Direct retrieval of canopy gap probability using airborne waveform lidar. *Remote Sens. Environ.* 134, 24–38. <https://doi.org/10.1016/j.rse.2013.02.021>.
- Armstrong, J., Tang, H., Hancock, S., Marselis, S., Duncanson, L., Kellner, J., Hofton, M., Blair, J.B., Fatoyinbo, T., Dubayah, R.O., 2020. AfriSAR: Gridded Forest Biomass and Canopy Metrics Derived from LVIS, Gabon, 2016. <https://doi.org/10.3334/ORNLDAAC/1775>.
- Asner, G.P., Mascaro, J., 2014. Mapping tropical forest carbon: Calibrating plot estimates to a simple LiDAR metric. *Remote Sens. Environ.* 140, 614–624.
- Asner, G.P., Mascaro, J., Muller-Landau, H.C., Vieilledent, G., Vaudry, R., Rasamoelina, M., Hall, J.S., Van Breugel, M., 2011. A universal airborne LiDAR approach for tropical forest carbon mapping. *Oecologia* 168, 1147–1160. <https://doi.org/10.1007/s00442-011-2165-z>.
- Bergen, K.M., Goetz, S.J., Dubayah, R.O., Henebry, G.M., Hunsaker, C.T., Imhoff, M.L., Nelson, R.F., Parker, G.G., Radeloff, V.C., 2009. Remote sensing of vegetation 3-D structure for biodiversity and habitat: Review and implications for lidar and radar spaceborne missions. *Journal of Geophysical Research: Biogeosciences* 114 (G2).
- Blair, J.B., Hofton, M.A., 1999. Modeling laser altimeter return waveforms over complex vegetation using high-resolution elevation data, 26, pp. 2509–2512.
- Blair, J.B., Hofton, M., 2018. AfriSAR LVIS L2 Geolocated Surface Elevation Product, Version 1. Boulder, Colorado USA. NASA National Snow and Ice Data Center Distributed Active Archive Center. <https://doi.org/10.5067/A0PMUXXVUYNH>.
- Blair, J.B., Rabine, D.L., Hofton, M.A., 1999. The Laser Vegetation Imaging Sensor: A medium-altitude, digitisation-only, airborne laser altimeter for mapping vegetation and topography. *ISPRS J. Photogramm. Remote Sens.* 54, 115–122. [https://doi.org/10.1016/S0924-2716\(99\)00002-7](https://doi.org/10.1016/S0924-2716(99)00002-7).
- Bürkner, P.-C., 2017. brms: An R Package for Bayesian Multilevel Models Using Stan. *J. Stat. Softw.* 1 (1) <https://doi.org/10.18637/jss.v080.i01>.
- Bustamante, M.M.C., Roitman, I., Aide, T.M., Alencar, A., Anderson, L.O., Aragão, L., Asner, G.P., Barlow, J., Berenguer, E., Chambers, J., Costa, M.H., Fanin, T., Ferreira, L.G., Ferreira, J., Keller, M., Magnusson, W.E., Morales-Barquero, L., Morton, D., Ometto, J.P.H.B., Palace, M., Peres, C.A., Silvério, D., Trumbore, S., Vieira, I.C.G., 2016. Toward an integrated monitoring framework to assess the effects of tropical forest degradation and recovery on carbon stocks and biodiversity. *Glob. Chang. Biol.* 22, 92–109. <https://doi.org/10.1111/gcb.13087>.
- Carreiras, J.M.B., Quegan, S., Le Toan, T., Ho Tong Minh, D., Saatchi, S.S., Carvalhais, N., Reichstein, M., Scipal, K., 2017. Coverage of high biomass forests by the ESA BIOMASS mission under defense restrictions. *Remote Sens. Environ.* 196, 154–162. <https://doi.org/10.1016/j.rse.2017.05.003>.
- Chave, J., Rejou-Mechain, M., Briquez, A., Chidumayo, E., Colgan, M.S., Delitti, W.B.C., Duque, A., Eid, T., Fearnside, P.M., Goodman, R.C., Henry, M., Martinez-Yrizar, A., Mugasha, W.A., Muller-Landau, H.C., Mencuccini, M., Nelson, B.W., Ngomanda, A., Nogueira, E.M., Ortiz-Malavassi, E., Pilissier, R., Ploton, P., Ryan, C.M., Saldarriaga, J.G., Vieilledent, G., 2014. Improved allometric models to estimate the aboveground biomass of tropical trees. *Glob. Chang. Biol.* 20, 3177–3190. <https://doi.org/10.1111/gcb.12629>.
- Cloude, S.R., Papathanassiou, K.P., 2003. Three-stage inversion process for polarimetric SAR interferometry. In: *IEEE Proc. - Radar, Sonar Navig.* 150, p. 125. <https://doi.org/10.1049/ip-rsn:20030449>.
- Denbina, M., Simard, M., Hawkins, B., 2018a. Forest height estimation using multibaseline polinsar and sparse lidar data fusion. In: *IEEE J. Sel. Top. Appl. Earth Obs. Remote Sens.* pp. 1–19. <https://doi.org/10.1109/JSTARS.2018.2841388>.
- Denbina, M., Simard, M., Riel, B.V., Hawkins, B.P., Pinto, N., 2018b. AfriSAR: Rainforest Canopy Height Derived from PolInSAR and Lidar Data, Gabon. <https://doi.org/10.3334/ornladaac/1589>.
- Dubayah, R., Blair, J.B., Goetz, S., Fatoyinbo, L., Hansen, M., Healey, S., Hofton, M., Hurlt, G., Kellner, J., Luthcke, S., Armston, J., Tang, H., Duncanson, L., Hancock, S., Jantz, P., Marselis, S., Patterson, P.L., Qi, W., Silva, C., 2020. The Global Ecosystem Dynamics Investigation: High-resolution laser ranging of the Earth's forests and topography. *Sci. Remote Sens.* 1, 100002. <https://doi.org/10.1016/j.srs.2020.100002>.
- Duncanson, L., Neuenschwander, A., Hancock, S., Thomas, N., Fatoyinbo, T., Simard, M., Silva, C.A., Armston, J., Luthcke, S.B., Hofton, M., Kellner, J.R., Dubayah, R., 2020. Biomass estimation from simulated GEDI, ICESat-2 and NISAR across environmental gradients in Sonoma County, California. *Remote Sens. Environ.* 242, 111779. <https://doi.org/10.1016/j.rse.2020.111779>.
- Fatoyinbo, T., Saatchi, S.S., Armston, J., Poulsen, J., Marselis, S., Pinto, N., White, L.J.T., Jeffery, K., 2018. AfriSAR: Mondah Forest Tree Species, Biophysical, and Biomass Data, Gabon, 2016. <https://doi.org/10.3334/ornladaac/1580>.
- Farr, T.G., Rosen, P.A., Caro, E., Crippen, R., Duren, R., Hensley, S., Kobrick, M., Paller, M., Rodriguez, E., Roth, L., Seal, D., 2007. The shuttle radar topography mission. *Reviews of geophysics* 45 (2).
- Fisher, A., Armston, J., Goodwin, N., Scarth, P., 2020. Modelling canopy gap probability, foliage projective cover and crown projective cover from airborne lidar metrics in Australian forests and woodlands. *Remote Sens. Environ.* 237, 111520. <https://doi.org/10.1016/j.rse.2019.111520>.
- Forêt Ressources Management, 2018. Vision stratégique et industrialisation de la filière bois dans les 6 pays du Bassin du Congo: Horizon 2030. Banque Africaine de Développement, Montpellier, France.
- Gower, S.T., Norman, J.M., 1991. Rapid estimation of leaf area index in conifer and broad-leaf plantations. *Ecology* 72, 1896–1900. <https://doi.org/10.2307/1940988>.
- Hajsek, I., Pardini, M., Horn, R., Scheiber, R., Jäger, M., Keller, M., Geßwein, D., Papathanassiou, K., Reigber, A., 2016. 3-D SAR Imaging of African Forests: Results from the AfriSAR Campaign at P- and L-Band, pp. 36–39.
- Hancock, S., Hofton, M., Sun, X., Tang, H., Kellner, J.R., Armston, J., Duncanson, L.L., Dubayah, R., 2019. The GEDI simulator: A large-footprint waveform lidar simulator for calibration and validation of spaceborne missions. *Earth Sp. Sci.* 1–17. <https://doi.org/10.1029/2018ea000506>.
- Hawkins, B.P., Pinto, N., Laval, M., Hensley, S., 2018. AfriSAR: Polarimetric Height Profiles by TomoSAR, Lope and Rabi Forests, Gabon. <https://doi.org/10.3334/ornladaac/1577>.
- Hensley, S., Wheeler, K., Sadowy, G., Jones, C., Shaffer, S., Zebker, H., Miller, T., Heavey, B., Chuang, E., Chao, R., Vines, K., 2008. The uavsar instrument: description and first results. In: 2008 IEEE Radar Conf, 31, pp. 1–6. <https://doi.org/10.1117/12.788949>.
- Hensley, S., Van Zyl, J., Laval, M., Neumann, M., Michel, T., Muellerschoen, R., Pinto, N., Simard, M., Moghaddam, M., 2015. October. L-band and P-band studies of vegetation at JPL. In: 2015 IEEE Radar Conference, pp. 516–520. IEEE.
- Houghton, R.A., 2005. Aboveground forest biomass and the global carbon balance. *Global change biology* 11 (6), 945–958.
- Kugler, F., Lee, S., Hajsek, I., Papathanassiou, K.P., 2015. Forest height estimation by means of Pol-InSAR data inversion: the role of the vertical wavenumber. *IEEE Trans. Geosci. Remote Sens.* 53, 5294–5311. <https://doi.org/10.1109/TGRS.2015.2420996>.
- Labrière, N., Tao, S., Chave, J., Scipal, K., Toan, T.L., Abernethy, K., Alonso, A., Barbier, N., Bissengou, P., Casal, T., Davies, S.J., Ferraz, A., Hérault, B., Jaouen, G., Jeffery, K.J., Kenfack, D., Korte, L., Lewis, S.L., Malhi, Y., Memiaghe, H.R., Poulsen, J.R., Réjou-Mechain, M., Villard, L., Vincent, G., White, L.J.T., Saatchi, S., 2018. In Situ reference datasets from the TropiSAR and AfriSAR campaigns in support of upcoming spaceborne biomass missions. In: *IEEE J. Sel. Top. Appl. Earth Obs. Remote Sens.* 11, pp. 3617–3627. <https://doi.org/10.1109/JSTARS.2018.2851606>.
- Laurance, W.F., Alonso, A., Lee, M., Campbell, P., 2006. Challenges for forest conservation in Gabon. *Central Africa. Futures* 38 (4), 454–470.
- Laval, M., Hensley, S., 2015. Extraction of structural and dynamic properties of forests from polarimetric-interferometric SAR data affected by temporal decorrelation. *IEEE Trans. Geosci. Remote Sens.* 53, 4752–4767. <https://doi.org/10.1109/TGRS.2015.2409066>.

- Lavalle, M., Shiroma, G.H.X., Agram, P., Gurrola, E., Sacco, G.F., Rosen, P., 2016. Plant: polarimetric-interferometric lab and analysis tools for ecosystem and land-cover science and applications. In: Lavalle, Marco, Shiroma, Gustavo H.X., Agram, Piyush, Gurrola, Eric, Sacco, Gian Franco, Rosen, Paul (Eds.), *Jet Propulsion Laboratory, Californ*, pp. 5354–5357.
- Lavalle, M., Riel, B.V., Shiroma, G., Hawkins, B.P., 2018. AfriSAR: Canopy Structure Derived from PolInSAR and Coherence TomoSAR NISAR tools. <https://doi.org/10.3334/orndaac/1601>.
- Le Toan, T., Quegan, S., Davidson, M.W.J., Balzter, H., Paillou, P., Papathanassiou, K., Plummer, S., Rocca, F., Saatchi, S., Shugart, H., Ulander, L., 2011. The BIOMASS mission: Mapping global forest biomass to better understand the terrestrial carbon cycle. *Remote Sens. Environ.* 115, 2850–2860. <https://doi.org/10.1016/j.rse.2011.03.020>.
- Lombardini, F., Reigber, A., 2003. Adaptive spectral estimation for multibaseline SAR tomography with airborne L-band data. In: *IGARSS 2003. 2003 IEEE International Geoscience and Remote Sensing Symposium. Proceedings (IEEE Cat. No. 03CH37477)* 3, 2014–2016. IEEE.
- MacArthur, R.H., Horn, H.S., 1969. Foliage Profile by Vertical Measurements. *Ecology* 50, 802–804. <https://doi.org/10.2307/1933693>.
- Malhi, Y., Adu-Bredu, S., Asare, R.A., Lewis, S.L., Mayaux, P., Malhi, Y., 2013. African rainforests: past, present and future. *Philos. Trans. R. Soc. B* 368.
- Marselis, S.M., Tang, H., Armston, J.D., Calders, K., Labrière, N., Dubayah, R., 2018. Distinguishing vegetation types with airborne waveform lidar data in a tropical forest-savanna mosaic: A case study in Lopé National Park. *Gabon. Remote Sens. Environ.* 216, 626–634. <https://doi.org/10.1016/j.rse.2018.07.023>.
- Marshak, C., Simard, M., Duncanson, L., Silva, C.A., Denbina, M., Liao, T.H., Fatoyinbo, L., Moussavou, G., Armston, J., 2020. Regional tropical aboveground biomass mapping with l-band repeat-pass interferometric radar, sparse lidar, and multiscale superpixels. *Remote Sens.* 12, 1–22. <https://doi.org/10.3390/rs12122048>.
- Medjibe, V.P., Putz, F.E., Romero, C., 2013. Certified and uncertified logging concessions compared in Gabon: changes in stand structure, tree species, and biomass. *Environmental management* 51 (3), 524–540.
- Ni-Meister, W., Yang, W., Kiang, N.Y., 2010a. A clumped-foliage canopy radiative transfer model for a global dynamic terrestrial ecosystem model. I: Theory. *Agric. For. Meteorol.* 150, 881–894. <https://doi.org/10.1016/j.agrformet.2010.02.009>.
- Ni-Meister, W., Lee, S., Strahler, A.H., Woodcock, C.E., Schaaf, C., Yao, T., Ranson, K.J., Sun, G., Blair, J.B., 2010b. Assessing general relationships between aboveground biomass and vegetation structure parameters for improved carbon estimate from lidar remote sensing. *J. Geophys. Res. Biogeosci.* 115.
- NISAR, 2018. NASA-ISRO SAR (NISAR) Mission Science Users' Handbook. Calif. Inst. Technol. Jet Propuls. Laboaroty 261.
- Papathanassiou, K.P., Cloude, S.R., 2004. The effect of temporal decorrelation on the inversion of forest parameters from Pol-InSAR data, pp. 1429–1431. <https://doi.org/10.1109/igarss.2003.1294134>.
- Pardini, M., Armston, J., Qi, W., Lee, S.K., Tello, M., Cazcarra Bes, V., Choi, C., Papathanassiou, K.P., Dubayah, R.O., Fatoyinbo, L.E., 2019. Early lessons on combining lidar and multi-baseline SAR measurements for forest structure characterization. *Surv. Geophys.* 40 <https://doi.org/10.1007/s10712-019-09553-9>.
- Poulsen, J.R., Koerner, S.E., Miao, Z., Medjibe, V.P., Banak, L.N., White, L.J.T., 2017. Forest structure determines the abundance and distribution of large lianas in Gabon. *Glob. Ecol. Biogeogr.* 26, 472–485. <https://doi.org/10.1111/geb.12554>.
- Pourshamsi, M., Garcia, M., Lavalle, M., Pottier, E., Balzter, H., 2018. Machine-learning fusion of PolSAR and LiDAR data for tropical forest canopy height estimation. In: *Int. Geosci. Remote Sens. Symp.* 2018-July, 8108–8111. <https://doi.org/10.1109/IGARSS.2018.8518030>.
- Quegan, S., Le Toan, T., Chave, J., Dall, J., Exbrayat, J.F., Minh, D.H.T., Lomas, M., D'Alessandro, M.M., Paillou, P., Papathanassiou, K., Rocca, F., Saatchi, S., Scipal, K., Shugart, H., Smallman, T.L., Soja, M.J., Tebaldini, S., Ulander, L., Villard, L., Williams, M., 2019. The European Space Agency BIOMASS mission: Measuring forest above-ground biomass from space. *Remote Sens. Environ.* 227, 44–60. <https://doi.org/10.1016/j.rse.2019.03.032>.
- Reigber, A., Moreira, A., 2000. First demonstration of airborne SAR tomography using multibaseline L-band data. *IEEE Transactions on Geoscience and Remote Sensing* 38 (5), 2142–2152.
- Réjou-Méchain, M., Tanguy, A., Piponiot, C., Chave, J., Hérault, B., 2017. Biomass: an R Package for Estimating Above-Ground Biomass and Its Uncertainty in Tropical Forests. *Methods Ecol. Evol.* 8, 1163–1167. <https://doi.org/10.1111/2041-210X.12753>.
- Riel, B., Denbina, M., Lavalle, M., 2018. Uncertainties in Forest Canopy Height Estimation From Polarimetric Interferometric SAR Data. *IEEE J. Sel. Top. Appl. Earth Obs. Remote Sens.* 11, 3478–3491. <https://doi.org/10.1109/JSTARS.2018.2867789>.
- Rosen, P., Hensley, S., Shaffer, S., Edelstein, W., Kim, Y., Kumar, R., Misra, T., Bhan, R., Satish, R., Sagi, R., 2016. An update on the NASA-ISRO dual-frequency DBF SAR (NISAR) mission. In: *2016 IEEE International Geoscience and Remote Sensing Symposium (IGARSS)*, pp. 2106–2108. <https://doi.org/10.1109/IGARSS.2016.7729543>.
- Rosen, P.A., Kim, Y., Kumar, R., Misra, T., Bhan, R., Sagi, V.R., 2017. Global persistent SAR sampling with the NASA-ISRO SAR (NISAR) mission. In: *2017 IEEE Radar Conf. RadarConf 2017*, pp. 0410–0414. <https://doi.org/10.1109/RADAR.2017.7944237>.
- Saatchi, S.S., Harris, N.L., Brown, S., Lefsky, M., Mitchard, E.T.A., Salas, W., Zutta, B.R., Buermann, W., Lewis, S.L., Hagen, S., Petrova, S., White, L., Silman, M., Morel, A., 2011. Benchmark map of forest carbon stocks in tropical regions across three continents. *Proc. Natl. Acad. Sci.* 108, 9899–9904. <https://doi.org/10.1073/pnas.1019576108>.
- Sannier, C., McRoberts, R.E., Fichet, L.V., Makaga, E.M.K., 2014. Using the regression estimator with landsat data to estimate proportion forest cover and net proportion deforestation in gabon. *Remote Sens. Environ.* 151, 138–148. <https://doi.org/10.1016/j.rse.2013.09.015>.
- Shiroma, G.H.X., Lavalle, M., 2020. Digital Terrain, Surface, and Canopy Height Models From InSAR Backscatter-Height Histograms. *IEEE Trans. Geosci. Remote Sens.* 58, 1–24. <https://doi.org/10.1109/tgrs.2019.2956989>.
- Silva, C.A., Saatchi, S., Garcia, M., Labriere, N., Klauber, C., Ferraz, A., Meyer, V., Jeffery, K.J., Abernethy, K., White, L., Zhao, K., Lewis, S.L., Hudak, A.T., 2018. Comparison of Small- and Large-Footprint Lidar Characterization of Tropical Forest Aboveground Structure and Biomass: A Case Study From Central Gabon. *IEEE J. Sel. Top. Appl. Earth Obs. Remote Sens.* 1–15. <https://doi.org/10.1109/JSTARS.2018.2816962>.
- Soja, M.J., Quegan, S., d'Alessandro, M.M., Banda, F., Scipal, K., Tebaldini, S., Ulander, L.M.H., 2021. Mapping above-ground biomass in tropical forests with ground-cancelled P-band SAR and limited reference data. *Remote Sens. Environ.* 253, 112153. <https://doi.org/10.1016/j.rse.2020.112153>.
- Tang, H., Armston, J., 2019. Algorithm Theoretical Basis Document (ATBD) for GEDI L2B Footprint Canopy Cover and Vertical Profile Metrics.
- Tang, H., Dubayah, R., 2017. Light-driven growth in Amazon evergreen forests explained by seasonal variations of vertical canopy structure. *Proc. Natl. Acad. Sci.* 114, 2640–2644. <https://doi.org/10.1073/pnas.1616943114>.
- Tang, H., Dubayah, R., Swatantran, A., Hofton, M., Sheldon, S., Clark, D.B., Blair, B., 2012. Retrieval of vertical LAI profiles over tropical rain forests using waveform lidar at La Selva, Costa Rica. *Remote Sens. Environ.* 124, 242–250. <https://doi.org/10.1016/j.rse.2012.05.005>.
- Tang, H., Armston, J., Hancock, S., Hofton, M., Blair, J.B., Fatoyinbo, T., Dubayah, R.O., 2018. AfriSAR: Canopy Cover and Vertical Profile Metrics Derived from LVIS, Gabon, p. 2016. <https://doi.org/10.3334/orndaac/1591>.
- Tebaldini, S., Rocca, F., Mariotti D'Alessandro, M., Ferro-Famil, L., 2016. Phase calibration of airborne tomographic SAR data via phase center double localization. *IEEE Trans. Geosci. Remote Sens.* 54, 1775–1792. <https://doi.org/10.1109/TGRS.2015.2488358>.
- Wasik, V., Dubois-Fernandez, P.C., Taillandier, C., Saatchi, S.S., 2018. The AfriSAR Campaign: Tomographic Analysis with Phase-Screen Correction for P-Band Acquisitions. *IEEE J. Sel. Top. Appl. Earth Obs. Remote Sens.* 11, 3492–3504. <https://doi.org/10.1109/JSTARS.2018.2831441>.
- Yu, Y., Saatchi, S., 2016. Sensitivity of L-band SAR backscatter to aboveground biomass of global forests. *Remote Sens.* 8 <https://doi.org/10.3390/rs8060522>.